



# Antibiotics Contaminated Irrigation Water: An Overview on Its Impact on Edible Crops and Visible Light Active Titania as Potential Photocatalysts for Irrigation Water Treatment

Ghadeer Jalloul<sup>1</sup>, Imad Keniar<sup>2</sup>, Ali Tehrani<sup>3</sup> and Cassia Boyadjian<sup>1\*</sup>

<sup>1</sup>Baha and Walid Bassatne Department of Chemical Engineering and Advanced Energy, Maroun Semaan Faculty of Engineering and Architecture, American University of Beirut, Beirut, Lebanon, <sup>2</sup>Department of Agriculture, Faculty of Agricultural and Food Sciences, American University of Beirut, Beirut, Lebanon, <sup>3</sup>Department of Bioproducts and Biosystems, Aalto University, Espoo, Finland

## OPEN ACCESS

### Edited by:

Chrysi S. Laspidou,  
University of Thessaly, Greece

### Reviewed by:

Ljubica Tasic,  
State University of Campinas, Brazil  
Xiaohui Liu,  
Chinese Research Academy of  
Environmental Sciences, China

### \*Correspondence:

Cassia Boyadjian  
cb30@aub.edu.lb

### Specialty section:

This article was submitted to  
Toxicology, Pollution and the  
Environment,  
a section of the journal  
Frontiers in Environmental Science

**Received:** 01 September 2021

**Accepted:** 29 November 2021

**Published:** 22 December 2021

### Citation:

Jalloul G, Keniar I, Tehrani A and  
Boyadjian C (2021) Antibiotics  
Contaminated Irrigation Water: An  
Overview on Its Impact on Edible  
Crops and Visible Light Active Titania  
as Potential Photocatalysts for  
Irrigation Water Treatment.  
*Front. Environ. Sci.* 9:767963.  
doi: 10.3389/fenvs.2021.767963

Sub-therapeutic levels of antibiotics (ABs) are given to animals and poultry to promote growth and reduce disease. In agricultural environments, ABs reach croplands via animal manure used as fertilizer and/or ABs-contaminated water used for irrigation. The continuous discharge of ABs into the ecosystem raises growing concerns on the ABs contamination of edible crops. Tetracyclines (TCs) are among the most widely used ABs around the world. In this review, we discuss the contamination of irrigation water with TCs, its impact on edible crops, and the potential risks of crop contamination with TCs on human health. We propose solar-mediated photocatalytic degradation using Titania (TiO<sub>2</sub>) photocatalyst as a promising method to remove TCs from irrigation water. The photocatalytic activity of TiO<sub>2</sub> can be enhanced by chemical modification to expand its activity under visible light irradiation. Herein, we aim for providing literature-based guidance on developing a visible light-active TiO<sub>2</sub>-based system to degrade TCs and other ABs in water streams. We include a summary of recent advances on this topic based on three main modification methods of Titania: metal/non-metal/mixed doping, composite formation, and heterojunction construction. Among the investigated photocatalysts, Fe<sub>2</sub>O<sub>3</sub>-TiO<sub>2</sub>/Fe-zeolite and the N-doped TiO<sub>2</sub>/rGO immobilized composite catalysts were found to be very efficient in the degradation of TCs under visible light irradiation (i.e., 98% degradation within 60 min). Most immobilized TiO<sub>2</sub> based composite systems exhibited improved performances and hence we highlight these as efficient, cost effective and ecofriendly photocatalysts for the degradation of TCs in irrigation water.

**Keywords:** antibiotics, crops, photocatalysis, TiO<sub>2</sub>, irrigation water

## 1 INTRODUCTION

Fresh water scarcity is an urgent global issue. Only (4%) of water on earth is fresh, and increasing global population, climate change, urbanization, and over exploitation continue to contaminate this scarce resource (Gothwal and Shashidhar, 2015). Pharmaceutical and organic chemical contamination of water is a critical threat to the natural ecosystem and public health (Zeghroud

et al., 2016). Amongst these pharmaceuticals, antibiotics (ABs) are a major concern (Anjali and Shanthakumar, 2019). ABs are natural or synthetic antimicrobial compounds used to treat bacterial infections in humans, animals, and plants by inhibiting or killing bacterial growth (Daghrir and Drogui, 2013; Anjali and Shanthakumar, 2019; Danner et al., 2019). ABs have efficacious applications in human and veterinary medicine; however, sub-therapeutic AB levels are routinely given to animals and poultry to promote growth (Gothwal and Shashidhar, 2015). In agricultural environments, these ABs reach croplands *via* animal manure used as fertilizer and/or the use of AB-contaminated irrigation water (Anjali and Shanthakumar, 2019; You et al., 2019).

The escalating use of ABs and their continuous discharge into the environment results in frequent detection of ABs in different environments, with concentrations of ng/L–mg/L in wastewater (Pan and Chu, 2017). Wastewater is commonly used for irrigating agricultural lands due to the scarcity of fresh water. There is evidence from greenhouse and field experiments that irrigating crops with ABs-contaminated water leads to crop contamination; studies performed on different edible crops (lettuce, cucumber, spinach, and pepper) using different groups of ABs detected these ABs in plant leaves and roots (Pan and Chu, 2017).

Bioaccumulation of ABs in edible crops and in water environments lead to potential risks to human health. The proliferation of ABs in the environment led to the emergence of antibiotic resistant bacteria and antibiotic resistance genes (Singh et al., 2019). Antibiotic resistance is defined as the ability of the target microbe to resist the action of the antibiotic drug that previously caused cell death. In human health, antibiotic resistant bacteria cause untreatable infections and increased mortality (Chen M. et al., 2019; Singh et al., 2019). Human consumption of ABs-contaminated edible crops and drinking water poses major health risks due to the potential antibiotic resistance transfer to human pathogens (Sponza and Koyuncuoglu, 2019). Current reports indicate that antibiotic resistance is an urgent health-threatening issue, causing 0.7 million deaths/year and estimated to grow to 10 million deaths by 2050 (Singh et al., 2019).

There are currently 250 different antibiotics classified in seven groups (Anjali and Shanthakumar, 2019). Tetracyclines are reported as the second most widely used AB group worldwide (Xu L. et al., 2021). Tetracyclines are a group of ABs that include chlortetracycline, oxytetracycline, tetracycline hydrochloride, and tetracycline (Daghrir and Drogui, 2013). Tetracyclines have gained specific attention due to their wide use in medical, agricultural, and poultry sectors, and due to their poor adsorption in humans and animals and high stability in soil and wastewater (Saadati et al., 2016a). For example (50–80%), of the tetracycline consumed by humans/animals is excreted through urine and feces, and they are stable in wastewater for 34–329 h due to their low volatility and high hydrophobicity (Daghrir and Drogui, 2013; Xu L. et al., 2021). Sources for tetracyclines discharge include pharmaceutical industries, farms, homes, and hospitals. Hence, the occurrence of these ABs in the environment is proportional to the economic status of the country and the size of the livestock and the pharmaceutical

industries. On the other hand, TCs discharge into the environment is also a consequence of the inefficiency of the current water treatment technologies used in removing these ABs (Christou et al., 2017; Pan and Chu, 2017). Particularly, tetracyclines are detected in the low ( $\mu\text{g/L}$ ) level in municipal wastewater, in the high ( $\mu\text{g/L}$ ) level in hospital wastewater, and in the (ng/L) level in underground, surface, and sea water (Homem and Santos, 2011). Although these concentrations appear low, they still impose risks to human health and the ecosystem *via* the potential development of antibacterial resistance (Danner et al., 2019).

Numerous studies have worked to develop efficient methods for removing ABs and specifically tetracyclines from water streams to eliminate potential threats to the ecosystem and humans (Saadati et al., 2016a; Minale et al., 2020). Removal technologies include adsorption, conventional technologies (biological processes, coagulation, flocculation, sedimentation, and filtration), membrane processes, chlorination, and advanced oxidation methods such as photolysis, electrochemistry, and photocatalysis (Homem and Santos, 2011; Wei et al., 2020). However, most of the conventional technologies such as the biological methods, filtration, coagulation/flocculation/sedimentation, and membrane processes suffer from the drawbacks of low efficiency, low degradation rate, incomplete mineralization, and high toxicity (Homem and Santos, 2011; Anjali and Shanthakumar, 2019). Solar light-activated photocatalytic degradation of ABs is an efficient, safe, residue-free, economical, and ecofriendly method to remove tetracyclines from wastewater, especially under visible light and ambient conditions (Homem and Santos, 2011; Wei et al., 2020). Various semiconductors and photocatalysts have been investigated for the photocatalytic degradation of tetracyclines including ZnO, TiO<sub>2</sub>, WO<sub>3</sub>, CdS, Fe<sub>3</sub>O<sub>4</sub>, g-C<sub>3</sub>N<sub>4</sub>, ZnS, and Bi<sub>2</sub>O<sub>3</sub> (Niu et al., 2013; Zhu et al., 2013; Zhang et al., 2014; Li et al., 2015; Vázquez et al., 2016; Wang T. et al., 2017; Yan et al., 2020). Semiconductors based on Titania (TiO<sub>2</sub>) are the most widely studied catalysts due to their low cost, high stability, low toxicity, good activity, and ease of modification (Teoh et al., 2012; Ibhaddon and Fitzpatrick, 2013; Koe et al., 2019; You et al., 2019; Zhang et al., 2019). However, the photocatalytic activity and application of TiO<sub>2</sub> is limited to the UV region of the light spectrum (200–400 nm), and further modifications are needed to expand its activity into the visible light region (400–700 nm). Recently, immense efforts have been dedicated for TiO<sub>2</sub> modification to expand its activity to the visible light region, and several modification methods and approaches have been reported (Basavarajappa et al., 2020).

This review discusses the escalating use of ABs; their continuous discharge into the agroecosystems contaminating both the soil and water; and the risks associated with using wastewater for crop irrigation. We present a summary of the latest literature studying the impact of ABs-contaminated irrigation water on the quality of edible crops and potential consequences for human health. Current research indicates that the use of ABs-contaminated irrigation water has potential risks to humans and ecosystems, and highlights an urgent need to develop efficient irrigation water treatment

technologies. Here, we focus on tetracyclines degradation under visible light using TiO<sub>2</sub>-based photocatalysts, and present a detailed summary of the latest advances in Titania modification to enhance its visible light activity for the photocatalytic degradation of tetracyclines in water. We identify the most efficient catalysts and discuss their advantages and disadvantages. For literature collection, we focused on studies investigating modified Titania-based catalysts for the photocatalytic degradation of tetracyclines under visible light irradiation between 2011 and 2021. We chose to discuss the three most reported modification methods; metal-nonmetal, mixed metal-nonmetal doping, TiO<sub>2</sub>-based composite formation, and TiO<sub>2</sub>-based heterojunction construction. For TCs presence in the environment, we adopted numerical data from recent studies which assessed the occurrence of TCs in various water media and their bioaccumulation in edible crops.

## 2 IMPACT OF ABs-CONTAMINATED IRRIGATION WATER ON EDIBLE CROPS AND POTENTIAL RISKS FOR HUMAN HEALTH

Fresh water scarcity has led to the reuse of wastewater for crop irrigation. Approximately  $20 \times 10^{10}$  m<sup>2</sup> of global agricultural land is irrigated with treated wastewater (Raschid-Sally and Jayakody, 2008). Countries that extensively use reclaimed water for irrigation include Australia, Columbia, United States, and China (Gudda et al., 2020). Conventional water treatment methods (coagulation, flocculation, sedimentation, and filtration) and biological treatment methods are only moderately effective in removing low concentrations of persistent organic contaminants such as antibiotics. Generally, these methods have very low efficiency in removing ABs from wastewater, and the efficiency depends on the physicochemical properties of the AB to be removed and the operating conditions of the treatment system (Pan et al., 2014; Christou et al., 2017). The use of reclaimed wastewater for crop irrigation introduces these organic contaminants into the soil and ultimately to crops.

Antibiotics have been detected in diverse edible crops. For example, in Minnesota, United States, sulfamethoxazole was detected in *Lactuca sativa* (lettuce) at concentrations of 100–1,200 µg/kg tissue (Christou et al., 2017). In Tianjin, China, tetracycline and sulfamethoxazole were detected in spinach and radish at concentrations of 6.3–330 µg/kg tissue (Hu et al., 2010). In the Pearl River delta, China, tetracyclines were detected in cabbage and *Ipomoea aquatica* (water spinach) at concentrations of 6.6 and 7.4 µg/kg tissue, respectively (Pan et al., 2014).

Several studies investigated the impact of ABs-contaminated irrigation water on the uptake of the crops of these contaminants. Both greenhouse (pot) and field experiments were reported. Herein, we present results of some of these experiments. In the summer of 2020, we conducted pot experiments to evaluate the accumulation of gentamicin and oxytetracycline

in three crops that are consumed fresh, including radish, lettuce, and cucumber (Imad Keniar et al., 2021). The crops were irrigated with 20 mg/L of each of the studied ABs. After harvesting, these ABs were detected in crop extracts using ELISA. The results detected gentamicin accumulation up to 13, 16, and 18 ng/g in cucumber, lettuce, and radish, respectively, whereas oxytetracycline accumulation was less than 3.0 ng/g in all three crops. Azanu et al. (Azanu et al., 2016) evaluated the accumulation of tetracycline and amoxicillin in potted lettuce and carrot irrigated with water containing known concentrations of 0.1–15 mg/L of tetracycline and amoxicillin. ABs were extracted from lettuce leaves and carrot tubers using accelerated solvent extraction, and then analyzed using liquid chromatography-tandem mass spectrometry. Tetracycline was detected in concentrations ranging between 4.4 and 28.3 ng/g in lettuce, and 12–36.8 ng/g in carrots. Whereas, amoxicillin was detected in concentrations ranging between 13.7 and 45.2 ng/g in both crops, which indicated that the amoxicillin uptake by lettuce and carrot was significantly higher than that of tetracycline. Hussein et al. (Hussain et al., 2016) conducted a field study in Lahore, Pakistan, which irrigated wheat, spinach, and carrot using pharmaceutical wastewater. The results showed that each of these crops accumulated 0–1 ng/g tissue of ciprofloxacin, ofloxacin, levofloxacin, oxytetracycline, and doxycycline.

Current data provide clear evidence that the use of ABs-contaminated irrigation wastewater can contaminate the soil and ultimately lead to ABs accumulation in edible crops. The extent of plant uptake of ABs from contaminated water depend on the type and concentration of the AB, its water solubility, sorption potential, and lipophilicity (Azanu et al., 2016). A clear understanding of AB bioaccumulation in crops and their ecotoxicological effects requires greater knowledge of the physicochemical properties of ABs in the soil and the mechanism of their translocation and bioaccumulation in plants (Pan and Chu, 2017). Field studies are necessary to accurately assess ABs uptake by various crops under different environmental conditions, and determine the impact of ABs accumulation in these crops (Pan and Chu, 2017).

Excessive use of treated wastewater in agriculture is increasing the risk of transmitting AB resistant pathogens/genes to the crops, which could potentially be transferred to the human microbiome through the food chain (Gudda et al., 2020). The level of this risk on human health will depend on the level of exposure to these contaminated crops through consumption. Pan et al. (Pan and Chu, 2017) proposed that human exposure to ABs through annual consumption of edible crops grown in manure-amended or wastewater-irrigated soil is likely to be low. For example, assessments of annual human exposure to different ABs through consumption of various crops in China indicated that consumption of corn and rice led to the highest AB exposure. The daily human exposure to tetracyclines, quinolones, and chloramphenicol was assessed as (0.34–2.77 µg) and (11.0–21.8 µg) *via* consumption of corn and rice, respectively. These values remained lower than the recommended acceptable daily intake (20–200 mg/day) of these ABs. However, a comprehensive analysis of the impact of AB-contaminated edible crops on human health is lacking. This would require

**TABLE 1** | Maximum detected tetracyclines concentrations in different environments and different countries (Pan and Chu, 2017).

Antibiotic	Wastewater ( $\mu\text{g/L}$ )	Soil ( $\mu\text{g/g}$ )	Manure ( $\mu\text{g/g}$ )	Biosolid ( $\mu\text{g/g}$ )	Plants ( $\mu\text{g/g}$ )
Tetracycline	254.820	0.178	43.500	0.513	0.0101
Country	Korean	Korean	China	Canada	China
Oxytetracycline	1.236	2.683	183.500	0.7436	0.330
Country	South Korean	China	China	United States	China
Chlortetracycline	444.20	107.9	268.00	0.3466	0.532
Country	Korean	China	China	United States	China

well-defined dietary studies to develop human exposure models and further integrate those models with disease outbreak analysis and clinical data. This will help estimate the relationship between the ingestion of AB resistant pathogens and their impact on human defense mechanisms and health (Pan and Chu, 2017; Sanganyado and Gwenz, 2019).

### 3 TETRACYCLINES OCCURRENCE IN WATER ENVIRONMENTS

This review focuses on the tetracyclines group as model ABs. Tetracyclines are one of the most prescribed ABs in human and animal infectious therapies due to their wide antimicrobial spectrum and low cost (Minale et al., 2020; Xu L. et al., 2021). Tetracyclines are extensively utilized as fertilizers and growth promoters in animal husbandry and agricultural industries (Daghrir and Drogui, 2013). Approximately (70%) of locally produced antibiotics are used for non-medical applications in the United States, and 4,200 tons of tetracyclines are utilized only in the agricultural industry (Xu L. et al., 2021). Tetracyclines have poor adsorption in humans/animals and high stability in soil and wastewater (Saadati et al., 2016a). For example (50–80%), of tetracyclines consumed by humans/animals are excreted through urine and feces, and after discharge into aquatic media, they are stable for 34–329 h due to their low volatility and high hydrophobicity (Daghrir and Drogui, 2013; Xu L. et al., 2021). AB contaminants are also persistent in soil and slowly degrade; for example, it took 90 days to degrade (44–75%) of the initial tetracycline concentration in a sterilized soil (Pan and Chu, 2017). Tetracyclines are released into the environment through animal manure, biosolids, sewage discharge, pharmaceutical wastewater, and the use of ABs-contaminated wastewater for irrigation (Pan and Chu, 2017). The AB concentration in each medium is directly related to the pollution source(s) and their distance from the medium. Tetracyclines are detected at low  $\mu\text{g/L}$  concentrations in municipal wastewater, at high  $\mu\text{g/L}$  concentrations in hospital wastewater, and at  $\text{ng/L}$  concentrations in underground, surface, and sea water (Homem and Santos, 2011). Although these concentrations seem rather low, they still carry risks for human health and the ecosystem through the development of antibiotic resistant bacteria and antibiotic resistance genes (Danner et al., 2019).

**Table 1** presents the maximum detected concentration ranges of tetracycline, oxytetracycline, and chlortetracycline in wastewater, soil, manure, biosolids, and plants in different countries. The highest concentrations of tetracycline and

chlortetracycline were detected in wastewater, whereas the highest concentration of oxytetracycline was in manure. The highest tetracycline concentrations detected in wastewater were tetracycline 254.820  $\mu\text{g/L}$  in Korea, chlortetracycline 44.420  $\mu\text{g/L}$  in Korea, and oxytetracycline 1.236  $\mu\text{g/L}$  in South Korea. The highest tetracyclines concentrations detected in soil, manure, and biosolids were 2.683, 183.500, and 0.7436  $\mu\text{g/g}$  of oxytetracycline, in China and United States. The highest tetracycline concentration detected in plant contamination was 0.532  $\mu\text{g/g}$  of chlortetracycline in China.

Several studies have investigated ABs contamination of surface water. **Table 2** presents the concentrations of tetracyclines in surface water streams in different countries. The predominant tetracycline detected in Ghana (Africa) was chlortetracycline, at concentrations of 0.044  $\mu\text{g/L}$ . In the Wangyang River in China, tetracycline was detected at 25.5  $\mu\text{g/L}$ . In Europe, the highest tetracycline concentration in surface water was detected in the United Kingdom, at a concentration of 1  $\mu\text{g/L}$ . In the United States, the highest concentration of tetracycline 102.7  $\mu\text{g/L}$  was detected in the Poudre River, Colorado. In Australia, the tetracycline concentration in surface water was minimal 0.008  $\mu\text{g/L}$ .

The varying levels of tetracycline contaminants in different countries reflect the scale of production and usage of tetracyclines in each country. This in turn is directly correlated to the economic development and industrial scale of the country. The highest concentrations of tetracyclines were detected in China, which is the biggest producer and consumer of ABs in the world. In 2013, China produced (248,000 tons) of ABs and consumed approximately (162,000 tons) (Zhang et al., 2015). China was the highest consumer of veterinary ABs in the livestock industry, reaching approximately (15,000 tons) in 2010 (Robles Jimenez et al., 2019). China will double its AB consumption in the livestock industry by 2030, when it will reach up to (35,000 tons) (Robles Jimenez et al., 2019). Tetracyclines were not detected in surface water in Lebanon (Mokh et al., 2017), likely due to the low scale of livestock activity. However, the latest Lebanese Ministry of Agriculture survey in 2009 reports rapid growth in livestock productivity (Mokh et al., 2020). Farmers use different groups of ABs to promote growth in cattle and poultry. Studies evaluating the presence of AB residues in cattle and poultry in different regions in Lebanon documented AB bioaccumulation in these animals. For example, a 2008 survey investigated the most widely used ABs in dairy cows from 26 random farms (more than 50% of them were small-scale farms with less than 1,000 cattle), and found wide use of streptomycin, gentamicin, penicillin, kanamycin, and oxytetracycline (Abi

**TABLE 2** | Maximum tetracyclines concentrations in different surface water streams in different countries (Danner et al., 2019; Singh et al., 2019).

Continent	Country	Antibiotic	Concentration ( $\mu\text{g/L}$ )
Africa	Ghana (rivers)	Tetracycline	0.03
	Ghana	Oxytetracycline	0.026
	Ghana	Chlortetracycline	0.044
Asia	Hong Kong	Tetracycline	0.0315
	China (Wangyang River)	Tetracycline	25.5
	China (Huangpu River)	Oxytetracycline	0.0845
	China	Chlortetracycline	0.017
Europe	Luxembourg (Alzette River)	Tetracycline	0.008
	United Kingdom	Tetracycline	1
	Spain	Tetracycline	0.228
	France	Tetracycline	0.007
	Poland (Drweca River)	Tetracycline	0.034
	Croatia	Chlortetracycline	0.43
	France	Chlortetracycline	0.68
	Luxembourg	Chlortetracycline	0.007
	Spain	Chlortetracycline	0.059
America	Cuba	Tetracycline	0.155
	United States (Poudre River)	Tetracycline	102.7
	Canada	Tetracycline	0.035
	Brazil	Tetracycline	0.011
	United States	Oxytetracycline	1.34
Australia	Australia (rivers)	Tetracycline	0.08

Khalil, 2008). Jammoul et al. (Jammoul and El Darra, 2019) evaluated ABs in 80 chicken muscle samples from different regions of Lebanon, and detected contaminating AB residues in (77.5%) of these samples. Ciprofloxacin (quinolones) represented the highest occurrence percentage (32.5%), followed by amoxicillin (lactams) (22.5%) and then tetracyclines (17.5%). The tetracyclines detected in these samples were below the maximum residue limit (MRL) values of 200  $\mu\text{g/kg}$  set by the Food and Agriculture Organization (FAO, 2018). There are no recent studies on AB bioaccumulation in edible crops and water environments in Lebanon.

## 4 PHOTOCATALYTIC DEGRADATION AS A POTENTIAL TREATMENT FOR CONTAMINATED IRRIGATION WATER

### 4.1 Photocatalysis

Antibiotics are stable in natural environments and persist in aquatic media because they are only partly biodegradable and are not completely removed by traditional wastewater treatment methods (only 24–36% removal efficiency) (Zeghioud et al., 2016; Pan and Chu, 2017). Hence, there is an urgent need to develop new technologies to detoxify wastewater streams by degrading these pharmaceuticals (Zeghioud et al., 2016). There are two main technologies to remove ABs from the environment: destructive and non-destructive methods.

Non-destructive methods include adsorption, liquid extraction, and membrane separation. Adsorption relies on solid and liquid phases, and the ability of the pollutant to move from the liquid phase to attach onto the solid adsorbent (Anjali and Shanthakumar, 2019). The adsorption efficiency depends

on the properties of the adsorbent, including its surface area, porosity, and pore diameter (Homem and Santos, 2011). Conventional treatments refer to methods that are utilized in water treatment plants, and include biological methods, filtration and coagulation/flocculation/sedimentation. In the biological systems, the organic compound degradation occurs in activated sludge tanks with the absence or presence of oxygen gas ( $\text{O}_2$ ) by monitoring the temperature and chemical oxygen demand. Filtration is the elimination of suspended solids in the feed by passing it over a granular solid medium, like sand, activated carbon, or coal. Coagulation/flocculation/sedimentation use particular chemicals like iron salts, polymers, lime, and alum to facilitate pollutant precipitation, particle sedimentation, and colloid generation to further collect them. (Homem and Santos, 2011). Membrane separation methods include reverse osmosis, nanofiltration, ultrafiltration, and ion exchange. These techniques do not degrade or remove contaminants, but entrap organic pollutants on filters (membranes) that require regeneration or disposal. The organic compounds and salts in contaminated wastewater affect the system performance and cause fouling of the membrane, leading to flux deterioration (Homem and Santos, 2011; Anjali and Shanthakumar, 2019). Ion exchange is based on anion and cation exchange between liquid and solid phases (sorbent/membrane), and is primarily used to improve water quality. It is rarely used to remove ABs from wastewater because this method requires ABs molecules to have ionizable groups (Homem and Santos, 2011).

Destructive methods include biodegradation and chemical oxidation processes (Calvete et al., 2019). Chemical oxidation processes include chlorination and advanced oxidation

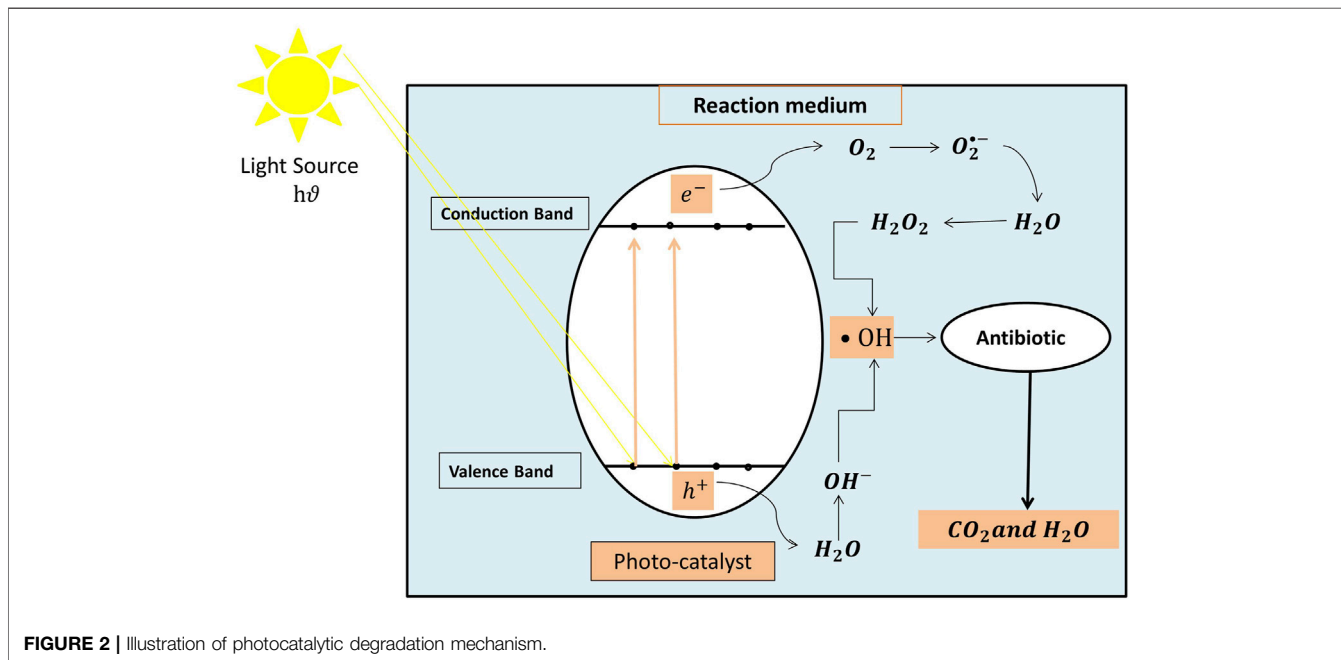
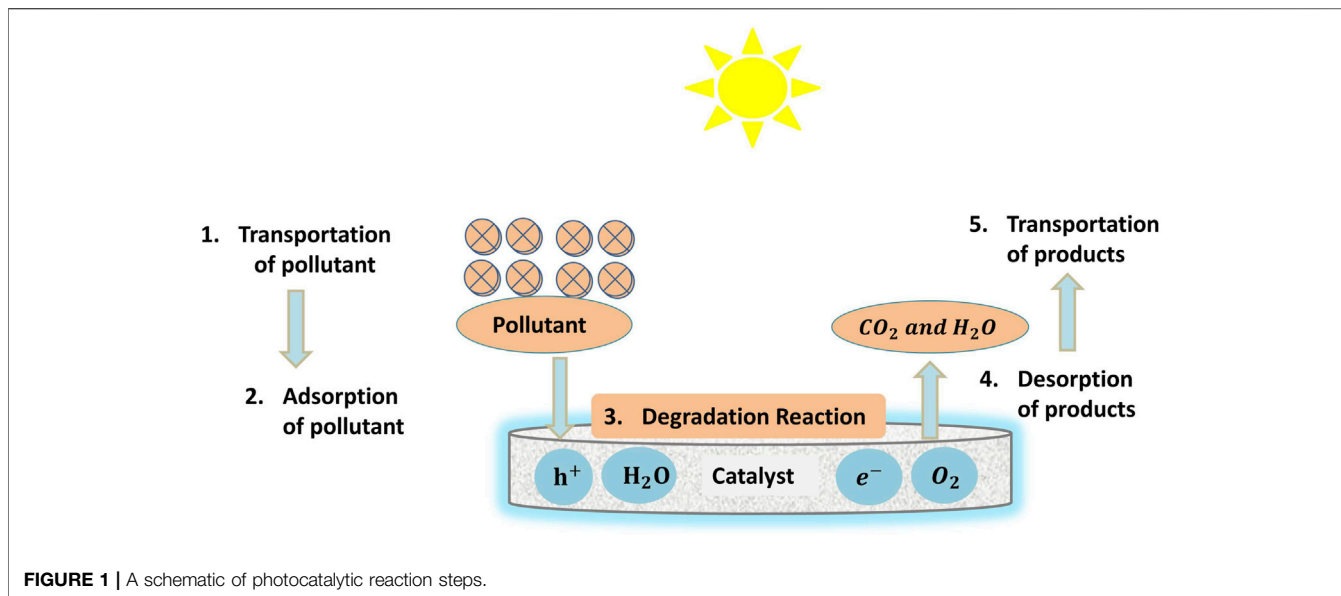
**TABLE 3** | Summary of methods for antibiotics removal from wastewater (Homem and Santos, 2011; Anjali and Shanthakumar, 2019).

Process	Advantages	Disadvantages	Examples of antibiotic
Adsorption	Can be applied to feeds with high concentrations of organic compounds and antibiotics	It only concentrates pollutants in the adsorbent medium that need to be treated or disposed of later. It is not widely used to remove tetracyclines from water	Oxytetracycline and Tetracycline Choi et al. (2008) Chlortetracycline Chen and Huang, (2010) Sulfamerazine Koyuncu et al. (2008)
Conventional	It can be applied to effluents with high flow rates	It has low removal efficiency and complex removal of coagulated pollutants. It is not applied to fluid streams with high pollutant concentrations due to its toxicity	Trimethoprim Kim et al. (2010) Sulfamethazine and Sulfadimethoxine Göbel et al. (2007)
Membrane technology (reverse osmosis, nano-filtration, and ultrafiltration)	Efficiently reduce high levels of dissolved salts. They do not require thermal energy	These methods are slow and inefficient when treating organic compounds such as pharmaceuticals. They are vulnerable to membrane fouling that reduces the efficiency	Sulfamethoxazole Radjenović et al. (2008) Sulfamerazine Adams et al. (2002) Oxytetracycline Kosutic et al. (2007)
Ion exchange	Reversible method that allows the resin or membrane to be reused after regeneration	Susceptible to fouling and requires backwashing. Rarely used for antibiotic removal	Sulfamethoxazole Tetracyclines Chlortetracycline Oxytetracycline Choi et al. (2007) Trimethoprim Adams et al. (2002)
Chlorination	Efficiently removes antibiotics from water containing low percentages of organic compounds	Its efficiency is function of the system pH. It can generate halogenated compounds, which are potentially carcinogenic	Amoxicillin and Erythromycin Navalon et al. (2008) Sulfamethoxazole Stackelberg et al. (2007) Sulfamerazine (Adams et al., 2002)
Photocatalysis	Can be applied under ambient conditions. Can save energy by utilizing solar light	Has not been industrialized due to the low light penetration in large-scale applications in slurry reactors. Difficult to remove and regenerate the catalyst	Amoxicillin Klauson et al. (2010) Lincomycin (Addamo et al., 2005) Tetracycline Zhu et al. (2013)
Electrochemical oxidation	Clean, easy, and effective method to remove high concentrations of antibiotics and toxic organic matter	Limited to small flow rates. Has high capital and operating costs	Lincomycin Carlesi Jara et al. (2007) Anthracyclines Hirose et al. (2005) Enrofloxacin Guinea et al. (2009)
Photolysis	Can be applied to wastewater containing photosensitive compounds and low chemical oxygen demand (COD) percentages	It is less effective than other techniques that use UV light along with catalysts or other additives. It is ineffective in treating wastewater contaminated with antibiotics	Penicillin Arslan-Alaton and Dogruel, (2004) Ciprofloxacin Vieno et al. (2007) Oxytetracycline Jiao et al. (2008)
Fenton and photofenton	These methods have good degradation percentages. They can be applied to wastewater with low COD concentrations	Photofenton cannot be applied to streams with high organic (pharmaceutical) contents due to water turbidity, which blocks light irradiation needed for catalyst activation. Sludge formation as function of the system pH remains challenging in these systems	Amoxicillin Zhang et al. (2006) Penicillin Arslan-Alaton and Dogruel, (2004) Lincomycin Bautitz and Nogueira, (2010)
Ozonation	It has acceptable pollutant degradation efficiency. It is suitable for the treatment of feeds with variable compositions	Expensive. Low mineralization percentage. High toxicity. High capital, operating, and maintenance costs	Amoxicillin Andreozzi et al. (2005) Sulfamethoxazole (Huber et al., 2003) Oxytetracycline Li et al. (2008)

processes. Chlorination oxidizes organic pollutants into less toxic and biodegradable compounds. This method uses low-cost gases such as chlorine and hypochlorite, and it is routinely used as a pretreatment for wastewater streams polluted with pharmaceutical contaminants that are to be treated in biological systems (Homem and Santos, 2011). Advanced oxidation processes oxidize organic pollutants using intermediate radicals such as hydroxyl radicals to transform them into less toxic and more biodegradable species. The intermediate radicals are very reactive, have lower selectivity than other oxidants, and are generated in the presence of ozone, hydrogen peroxide, ultraviolet radiation, or semiconductor photocatalyst (Homem and Santos, 2011). Examples of advanced oxidation processes include ozonation, fenton, and photofenton oxidation, photolysis, electrochemical technologies, and photocatalysis.

The most studied AB removal technologies include ozonation, fenton/photofenton oxidation, photolysis, photocatalysis,

electrochemical oxidation, chlorination, ion exchange, membrane technologies, and adsorption (Anjali and Shanthakumar, 2019; Homem and Santos, 2011). **Table 3** presents the advantages and disadvantages of each method. Photocatalysis is considered an environmentally friendly and low cost detoxification technique due to its utilization of solar light and complete mineralization of organic pollutants without generating residual waste or sludge (Sundar and Kanmani, 2020). Complete mineralization of the pollutant converts it into harmless species such as water, carbon dioxide, nitrogen, and other by-products, which in most cases are nontoxic (Zeghioud et al., 2016). The potential toxicity of products generated by photocatalytic degradation can be minimized by achieving high photocatalytic-induced mineralization (>99%) (Libralato et al., 2020). Bouafia-Chergui et al. (Bouafia-Chergui et al., 2016) studied the toxicity of products generated by photocatalytic degradation



of tetracycline by TiO<sub>2</sub> under UV light. The toxicity was evaluated by observing variations in the natural luminescent emissions of *Vibrio fischeri*. The results showed that the photoproduct toxicity increased after 240 min (from 60 to 84% inhibition of luminescence), then decreased to the minimum value after 360 min (35% inhibition of luminescence). This result indicated that total mineralization of tetracycline produced photoproducts with lower toxicity than tetracycline (Bouafia-Chergui et al., 2016).

The main components of photocatalysis systems are the light source, the photocatalyst, and the polluted water (Sundar and Kanmani, 2020). AB degradation *via* photocatalysis follows five

steps, as depicted in **Figure 1**: 1) diffusion of the organic pollutant from the bulk of the solution to the surface of the catalyst, 2) adsorption of the organic pollutant onto the surface of the catalyst, 3) degradation of the contaminants on the surface of the catalyst, 4) desorption of the resultant products from the surface of the photocatalyst, and 5) diffusion of the products from the surface of the semiconductor toward the bulk of the solution (Ibhadon and Fitzpatrick, 2013). After illumination by UV/visible light, the semiconductor (e.g., TiO<sub>2</sub>) molecules form unlinked pairs of electrons (e<sup>-</sup>)/holes (h<sup>+</sup>) due to the excitation of the electrons from the valence band (VB) to the conduction band (CB). These

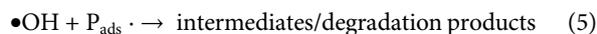
charge carriers may either return to the initial state in the semiconductor, or move to the surface of the catalyst to undergo various redox reactions with water molecules, hydroxide ions, and the pollutant. **Figure 2** illustrates the mechanism of photocatalysis, and **Eqs 1–6** define the chemical reactions. In these Equations,  $\text{TiO}_2$  represents the catalyst,  $(e^-)$  represents the conduction band electron, and  $(h^+)$  represents the valence band hole (Zeghioud et al., 2016).



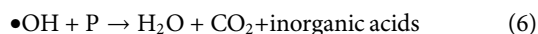
The positive hole  $(h^+)$  can produce hydroxyl radicals *via* two paths. The first path is hole transfer to the water molecule; the second path is hole transfer to a hydroxyl ion (**Eqs 2, 3**, respectively) (Zeghioud et al., 2016).



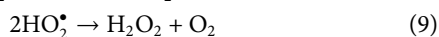
The positive hole  $(h^+)$  can also oxidize the antibiotic pollutants (P) in water (**Eq. 4**), followed by the formation of intermediates produced from reactions with the hydroxyl radicals (**Eq. 5**) (Zeghioud et al., 2016).



$\bullet\text{OH}$  radicals also can react with water pollutants to cause mineralization into water and carbon dioxide (**Eq. 6**) (Zeghioud et al., 2016).



In the presence of molecular oxygen, the excited electrons interact with the adsorbed oxygen on the catalyst surface (**Eq. 7**) and produce superoxide radicals ( $\text{O}_2^{\bullet-}$ ). These radicals are capable of preventing the recombination of the electrons with the positive holes (Zeghioud et al., 2016; Ibhaddon and Fitzpatrick, 2013) and are converted to hydrogen peroxide and then to hydroxyl radicals as shown in the (**Eqs 8–10**) (Homem and Santos, 2011). Hydroxyl radicals play a significant role in the degradation of the organic pollutant.



Many factors influence the efficiency of the photocatalytic degradation of various organic pollutants in water, including the concentrations of the contaminant and the catalyst, the light source and its intensity, the solution pH, the solution turbidity, the presence of other contaminants, and the type of photo-reactor employed (Saadati et al., 2016a). Increasing the initial AB or catalyst concentration increases the rate of degradation until reaching an optimal value, after which the degradation rate decreases (Saadati et al., 2016a). A suitable light source with an appropriate intensity and wavelength is essential to ensure optimum catalyst activation (Liu et al., 2013; Saadati et al., 2016a; Zhang et al., 2019). The effect of pH is a function of the operating

conditions and the chemical nature of pollutants and catalyst. The capacity of the catalyst itself to harvest light photons and efficiently utilize the excited electrons in degrading the pollutant is a critical factor that affects system performance (Saadati et al., 2016a). The water turbidity also affects photocatalysis efficiency. For example, high water turbidity in the treated stream can reduce light transmission through the water into the catalyst's surface, thereby reducing light absorption by the catalyst and subsequent electron activation (Teoh et al., 2012; Divakaran et al., 2021). The presence of salts and other organic pollutants in the water may affect AB adsorption onto the catalyst surface, and can increase water turbidity. Ghoreishian et al. (Ghoreishian et al., 2021) compared the performance of Fe and Sn co-doped- $\text{TiO}_2$  nanofibers for tetracycline degradation in synthetic, river, and tap water samples. The results showed that the highest efficiency was obtained for synthetic pure water (96.96%), followed by tap water (81.85%), and then river water (60.59%). This result clearly indicates that photocatalyst performance can be overestimated by experiments that use pure water in laboratory settings.

The choice of photocatalytic reactor is a function of the reaction system, including the chemical structure and concentrations of pollutants and catalyst, the operating flowrate, temperature, and pressure (Ibhaddon and Fitzpatrick, 2013). Slurry reactors are conventional reactors that suspend the heterogeneous photocatalysts in a liquid phase in the reactor. Heterogeneous photocatalysts are preferred over homogeneous photocatalysts in slurry reactors because they offer easier catalyst recovery and high efficiency. Accordingly, catalyst immobilization on solid substrates such as polymers, glass, sand, or reactor walls has been receiving great attention recently to achieve efficient catalyst recovery and sustainable system operation (Ibhaddon and Fitzpatrick, 2013; Zeghioud et al., 2016).

## 4.2 Photocatalytic Degradation of Tetracyclines

Tetracyclines contamination of surface and ground water, hence eventually irrigation water, is due to the inefficient removal capacity of current conventional wastewater plants, leading to residual tetracycline concentrations of up to 2.37  $\mu\text{g/L}$  in the final effluent stream released into the environment (Daghrir and Drogui, 2013). Photocatalytic degradation of tetracyclines using UV, visible, and solar light has been explored for complete tetracycline demineralization (Bouafia-Chergui et al., 2016; Chen et al., 2016; Farhadian et al., 2019). Three primary photocatalytic systems have been extensively studied: semiconductor systems such as  $\text{TiO}_2$  (Zhu et al., 2013; Niu et al., 2014; Safari et al., 2014) and  $\text{ZnO}$  (Farhadian et al., 2019); binary composite systems such as  $\text{Ag-Bi}_2\text{WO}_6$ ,  $\text{Ag-BiVO}_4\text{-Cu}_2\text{O}$ , and  $\text{AgBr-Ag}_3\text{PO}_4$  (Deng et al., 2017; Shen et al., 2018; Yan et al., 2018; Rasheed et al., 2019); and heterojunctions such as  $\text{AgI/WO}_3$ ,  $\text{CQDs/Bi}_2\text{WO}_6$ ,  $\text{C}_3\text{N}_4/\text{Bi}_2\text{WO}_6$ , and  $\text{CQDS/ZnO}$  (Di et al., 2015; Wang et al., 2016; Chen et al., 2017; Li J. et al., 2019).

Other common examples on materials used for tetracyclines photocatalytic degradation under both UV and visible light

**TABLE 4** | Previous work on tetracycline removal by TiO<sub>2</sub> catalyst under UV light.

#	Catalyst	TC initial concentration (mg/L)	Catalyst concentration (g/L)	UV light source	pH	Removal efficiency	Year and ref
1	TiO <sub>2</sub> P25 (Degussa) 20–30 nm	40	1	UV: 300 W (290 < λ < 365) mercury lamp	4.2	95% after 60 min	2013 Zhu et al. (2013)
2	Commercially available TiO <sub>2</sub> (BIOCHEM ChemoPharma)	5	2	UV: 12 W halogen lamp <sup>a</sup>	Free	100% after 210 min	2016 Bouafia-Chergui et al. (2016)
3	TiO <sub>2</sub> (US-Research Nanomaterials) 10–25 nm	15	2	UV: 15 W <sup>a</sup>	5	100% after 45 min	2018 Fazilati et al. (2018)

<sup>a</sup>Light wavelength was not specified in the original paper.

Free pH: medium pH was not controlled.

include the application and modification of titania (TiO<sub>2</sub>) semiconductors. In these studies, both high performance liquid chromatography (Wang et al., 2011; Cao et al., 2016) or UV–VIS spectrophotometer (Yu et al., 2014; Oseghe and Ofomaja, 2018a; Lyu et al., 2019; Ghoreishian et al., 2020) were used for the analysis of the water samples and for the evaluation of the degradation efficiency of the TCs over the investigated photocatalysts. Photocatalytic tetracycline degradation mediated by TiO<sub>2</sub> is expected to proceed *via* the formation of intermediates, which eventually completely degrade into CO<sub>2</sub>, H<sub>2</sub>O, and NH<sub>4</sub><sup>+</sup>. Zhu et al. (Zhu et al., 2013) proposed that TiO<sub>2</sub>-mediated tetracycline degradation involved electron transfer, hydroxylation, open-ring reactions, and cleavage of the central carbon.

### 4.3 TiO<sub>2</sub>-Based Photocatalysts for Tetracyclines Degradation

TiO<sub>2</sub> is the most studied and used heterogeneous photocatalyst semiconductor due to its super quantum yield (ratio of emitted photons to absorbed photons), low cost, non-toxicity, hydrophilicity, high photoactivity, interesting charge transport properties, and good chemical and photostability (Ibhadon and Fitzpatrick, 2013; Sommer et al., 2015; Koe et al., 2019; You et al., 2019; Zhang et al., 2019). TiO<sub>2</sub> exists in three polymorphs/crystal forms: anatase, rutile, and brookite. Anatase and rutile forms of TiO<sub>2</sub> are utilized as photocatalysts; however, anatase is preferred due to its superior quantum yield (Koe et al., 2019). A hybrid form of TiO<sub>2</sub> called Degussa (Evonik–Degussa) P-25 consists of a phase-junction mixture of (25%) rutile and (75%) anatase. TiO<sub>2</sub>-P25 is widely investigated for photodegradation of organic pollutants due to its availability, stability, reusability, and high oxidation activity compared to other crystal forms of TiO<sub>2</sub> (Ibhadon and Fitzpatrick, 2013; Koe et al., 2019).

TiO<sub>2</sub> has a band gap (E<sub>g</sub>) of approximately 3–3.2 eV, which limits its photoactivity to ultraviolet light with a wavelength less than 387 nm (Koe et al., 2019). **Table 4** summarizes some applications of Titania for photodegradation of tetracyclines under UV light. In general, Titania achieves very high degradation efficiencies of (95–100%) in relatively short periods of time (45–60 min).

Despite its promising photocatalytic activities, Titania has some shortcomings that limit its wide application in photocatalysis. For example, due to its wide band gap energy

(3.2 eV) TiO<sub>2</sub> can only be activated under UV light which only accounts for (5%) of the solar spectrum. The recombination rate of the charge carriers is significantly high in TiO<sub>2</sub>, and this suppresses its AB degradation efficiency. TiO<sub>2</sub> also undergoes agglomeration and aggregation which complicates its recovery and reuse in large-scale applications. Moreover, TiO<sub>2</sub> has low adsorption capacity of nonpolar contaminants due to its polar nonporous surface (Bahadar Khan and Kalsoom, 2019; Li R. et al., 2020).

Further modification of Titania is urgently needed to achieve practical, visible light-induced photocatalytic applications. Many studies have been reported in the literature to enhance Titania properties through modification and/or combination with organic and/or inorganic counterparts (Wang et al., 2011; Chen et al., 2016; Pouretedal and Afshari, 2016; Zhang S. et al., 2017; Zhang F. J. et al., 2017; Chen and Liu, 2017; Jin et al., 2017; Duan et al., 2018; He et al., 2018; Tang et al., 2018; Zheng et al., 2018; Liu M. et al., 2019; Chen Y. et al., 2019; Farhadian et al., 2019; Galedari et al., 2019; Sun et al., 2019; Akel et al., 2020; Zhang T. et al., 2020; Ghoreishian et al., 2020; Liu et al., 2020; Divakaran et al., 2021; Ghoreishian et al., 2021). The following section presents a detailed summary of various methods reported in the literature to achieve visible light sensitization of Titania and its applications for tetracyclines photodegradation.

## 5 MODIFICATION OF TiO<sub>2</sub> FOR ENHANCED VISIBLE LIGHT ACTIVITY

Researchers have studied TiO<sub>2</sub> modification for more than 30 years to enhance its visible light photocatalytic properties, stability, and reusability using three primary modification methods: 1) hinder the recombination of excited electrons and positive holes; 2) expand titania activity from the UV light spectrum to include visible light (accounts for approximately (43%) of the solar light spectrum) and ultimately solar light; and 3) enhance TiO<sub>2</sub> morphology, surface area, and ease of recovery (Teoh et al., 2012). Recent advances in titania modification include doping with metals and nonmetals, developing hybrid composite systems, and constructing heterojunction photocatalysts (Li and Shi, 2016). Each of

**TABLE 5** | Previous studies investigating tetracyclines removal by metal, nonmetal, and mixed metal-nonmetal doped TiO<sub>2</sub> catalysts.

#	Modified titania	TC initial concentration (mg/L)	Catalyst concentration	Light source	pH	Results with doped TiO <sub>2</sub>	Results with pure TiO <sub>2</sub>	Year and ref
1	Co-doped TiO <sub>2</sub>	30 Oxy-(TCH)	0.5 g/L	UV/vis illumination <sup>a</sup>	5	98% after 60 min	97% after 60 min	2020 Akel et al. (2020)
2	Zr/Sn co-doped TiO <sub>2</sub>	20 (TC)	0.8 g/L	36 W mercury low pressure lamp <sup>a</sup>	3	100% after 180 min	79% after 180 min	2015 Pouretedal and Afshari, (2016)
3	Fe/Sn co-doped TiO <sub>2</sub>	30 (TC)	0.3 g/L	300 W Xenon (Xe) arc lamp ( $\lambda > 420$ nm)	6	96.96% after 60 min	5% after 60 min	2021 Ghoreishian et al. (2021)
4	H <sub>2</sub> O <sub>2</sub> modified Zn-doped TiO <sub>2</sub>	80 (TC)	1 g/L	500 W Xe lamp <sup>a</sup>	7	88.14% after 360 min	70% after 360 min	2016 Pang et al. (2016)
5	Y <sup>3+</sup> /TiO <sub>2</sub> Hal-PMPD	50 (TC)	2 g/L	500 W Xe lamp ( $\lambda > 380$ nm)	1	78.8% after 50 min	–	2014 Yu et al. (2014)
6	Phosphorous-doped anatase TiO <sub>2</sub>	60 (TCH)	0.5 g/L	500 W halogen-tungsten lamp <sup>a</sup>	7	93% after 120 min	62% after 120 min (anatase)	2014 Niu et al. (2014)
7	C-N-S tri-doped TiO <sub>2</sub>	5 (TC)	0.5 g/L	6 W (F6T5/D) cold white visible lamp ( $\lambda > 420$ nm)	9	95% after 180 min	25% after 180 min	2011 Wang et al. (2011)
8	TiO <sub>2</sub> doped with acetylene black	10 (TCH)	0.5 g/L	30 W LED lamp (400 < $\lambda$ < 780 nm)	4.1	93.3% after 120 min	20% after 120 min	2020 Zhang T. et al. (2020)
9	N-doped TiO <sub>2</sub>	10 (TC)	0.2 g/L	Visible light ( $\lambda = 420$ nm)	7	90% after 120 min	73% after 120 min	2020 Wu et al. (2020)
10	Porous N, S co-doped TiO <sub>2</sub>	20 (TC)	0.4 g/L	300 W Xe lamp ( $\lambda > 420$ nm)	Free	84.9% after 60 min	Comparable results as modified	2020 Ouyang and Ji, (2020)
11	(Sn, Zn) and N co-doped TiO <sub>2</sub>	35 (TC)	0.5 g/L	Simulated solar irradiation <sup>a</sup>	7	33% after 120 min	22% after 120 min	2018 Riboldi et al. (2018)

<sup>a</sup>Light wavelength was not specified in the original paper.

Free pH: medium pH was not controlled.

Abbreviations: TC, tetracycline; TCH, tetracycline hydrochloride.

these Titania modification methods is discussed in the following sections.

## 5.1 Metal and Nonmetal Doping of TiO<sub>2</sub>

Doping is the introduction of a metallic and/or nonmetallic element (dopant) into the bulk of a semiconductor without modifying its structure or altering its crystallographic form (Teoh et al., 2012; Ibhaddon and Fitzpatrick, 2013). The presence of the dopant results in a large dipole moment that can alter the kinetics of the electron transfer process. It lowers the band gap energy and widens the light absorption spectrum by increasing the number of migrating electrons from the valence band to the conduction band of the main semiconductor (Koe et al., 2019). Consequently, optimal doping conditions enable photocatalyst activation under UV and visible light (380 nm <  $\lambda$  < 500 nm) (Ibhaddon and Fitzpatrick, 2013). Studies have investigated various dopants for the visible light sensitization of titania, including metal, nonmetal, or mixed metal-nonmetal doping (Li and Shi, 2016). The development of optimum doping conditions must consider the preparation method, the dopant concentration, and the type of dopant to ensure enhanced photocatalytic performance (Marschall and Wang, 2014). **Table 5** presents examples of the best performing metal, nonmetal, and mixed metal-nonmetal doping of TiO<sub>2</sub> photocatalysts and their performance in tetracyclines photodegradation under visible light.

### 5.1.1 Metal Ion Doping of TiO<sub>2</sub>

Metal ion dopants of Titania include transition, rare earth, and precious metal ions. Metal doping of Titania is achieved by

firing at high temperature or auxiliary deposition techniques (Zhang et al., 2019). **Figure 3** illustrates the mechanisms of tetracyclines degradation by metal-doped TiO<sub>2</sub> photocatalysts. Under visible light, electrons in the band gap energy of the doping metal are excited into the metal conduction band, and then move into the conduction band of the bulk catalyst. Simultaneously, Titania electrons are excited by the UV light of the solar light spectrum (**Eq. 1**). Consequently, these electron/hole pairs lead to a series of oxidation-reduction reactions that produce oxygen and hydroxyl radicals (**Eqs 2, 3, 7, 8, 9, 10**) which in turn degrade the AB molecules (**Eqs 4, 5, 6**). An example of an efficient transition metal-doped Titania is cobalt (Co)-doped TiO<sub>2</sub>, which has been used with and without immobilization on reduced graphene oxide surfaces for tetracycline and oxytetracycline removal, respectively (Jamali Alyani et al., 2019; Akel et al., 2020). Cobalt-doped Titania was prepared using the reflux method (Co-TiO<sub>2</sub>-R) by Akel et al. (Akel et al., 2020), and resulted in (98%) degradation of oxytetracycline hydrochloride (Oxy-TCH) under UV-visible light illumination. The authors attributed the high initial rate of Co-TiO<sub>2</sub>-R to its high surface area and enhanced charge transfer and separation properties imposed by impurity levels in the band gap energy; the Co particles entrapped some of the generated ( $h^+$ ), thereby minimizing the possibility of electron/hole recombination.

Metal co-doping was recently used to enhance visible light harvesting in TiO<sub>2</sub> catalysts. Co-doping resulted in higher visible light activity than that resulting from single-doping due to a

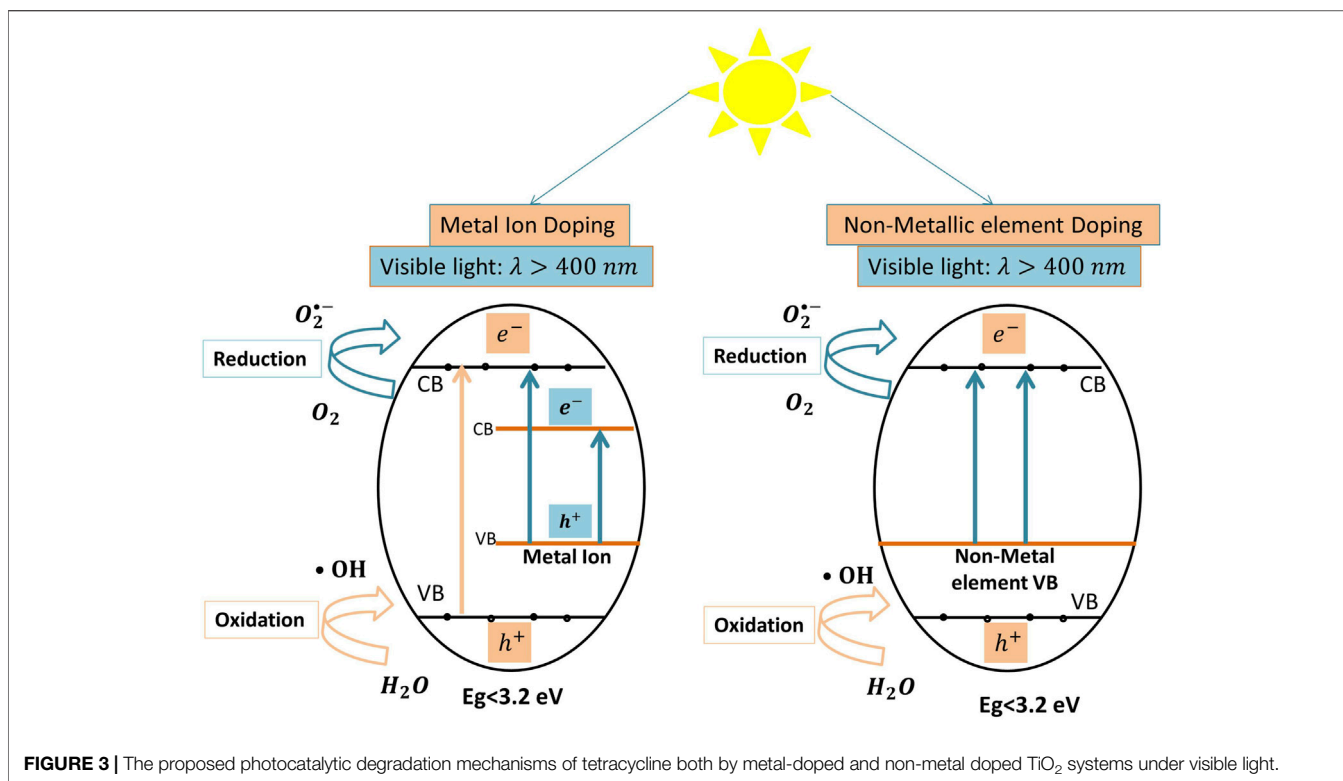


**FIGURE 3** | The proposed photocatalytic degradation mechanisms of tetracycline both by metal-doped and non-metal doped  $\text{TiO}_2$  systems under visible light.

synergistic effect between the two dopants (You et al., 2019). Recent studies investigated bimetallic doping of  $\text{TiO}_2$  for tetracyclines degradation using zirconium (Zr) and tin (Sn) (Pouretedal and Afshari, 2016), and iron (Fe) and tin (Sn) (Ghoreishian et al., 2021). Ghoreishian et al. (Ghoreishian et al., 2021) developed highly efficient Fe-Sn co-doped  $\text{TiO}_2$  nanofibers (Fe/Sn- $\text{TiO}_2$  NFs). Fe/Sn- $\text{TiO}_2$  NFs were produced using the electrospinning method, and then used for tetracycline degradation under 300 W xenon (Xe) lamp as the visible light source (Ghoreishian et al., 2021). This co-doped  $\text{TiO}_2$  catalyst displayed a very high photocatalytic degradation efficiency (96.96%), which was 1.86, 1.8, and 1.56 times higher than the efficiencies of unmodified  $\text{TiO}_2$ , Fe-doped  $\text{TiO}_2$ , and Sn-doped  $\text{TiO}_2$ , respectively. The authors attributed the enhanced performance of the co-doped catalyst to its small crystal size, tunable and low band gap energy, higher adsorption capability, better visible light absorption, enhanced charge carrier separation, and suppressed charge carrier recombination. This co-doped catalyst also displayed high stability and maintained (92%) degradation efficiency after five cycles of use. Total organic carbon (TOC) analysis was used to assess the extent of AB mineralization achieved by the catalyst. The Fe/Sn- $\text{TiO}_2$  NFs achieved (98%) tetracycline mineralization, compared to only (56%) tetracycline mineralization by the unmodified  $\text{TiO}_2$  catalyst.

### 5.1.2 Nonmetal Doping of $\text{TiO}_2$

Nonmetal doping has been investigated for the visible light activation of  $\text{TiO}_2$  (Farhadian et al., 2019; Niu et al., 2014; Oseghe and Ofomaja, 2018a; Tang et al., 2018; Chen and Liu,

2016; Wu et al., 2020; Fang et al., 2019; Oseghe and Ofomaja, 2018b). Nonmetal-doped photocatalysts display higher stability and better photoactivity than metal-doped photocatalysts because metal-doping of  $\text{TiO}_2$  can, for example in some applications, lower the doped catalyst stability, reduce its activity, and decrease its photo-quantum efficiency due to rapid recombination of the electrons and the holes (Teoh et al., 2012). Nonmetal dopants of  $\text{TiO}_2$  include nitrogen (N) (Farhadian et al., 2019; Wang et al., 2011; Tang et al., 2018; Chen and Liu, 2016; Wu et al., 2020), sulfur (S) (Wang et al., 2011), carbon (C) (Zhang T. et al., 2020), and phosphorous (P) (Niu et al., 2014). Nonmetal doping is performed by creating mid-gap energy levels between the valence and conduction bands of the parent catalyst (Zhang et al., 2019; Ibadon and Fitzpatrick, 2013; Radwan et al., 2018). The nonmetal dopant can enhance the visible light-induced photocatalytic activity of the catalyst because electrons in the newly created energy level can be excited by visible light into the conduction band of the bulk catalyst (Eq. 1). Eventually, these excited electrons settle on the surface of the doped catalyst and generate active radicals *via* redox reactions (Eqs 2, 3, 7, 8, 9, 10), which consequently attack and mineralize the AB molecules (Eqs 4, 5, 6) (Ibadon and Fitzpatrick, 2013; Radwan et al., 2018). Importantly, the nonmetal dopant inhibits the recombination of the charge carriers, due to electron entrapment by the oxygen vacancies created in the catalyst (Feng et al., 2018; Basavarajappa et al., 2020). **Figure 3** illustrates the mechanism of tetracyclines degradation by nonmetal-doped  $\text{TiO}_2$  systems.

Nitrogen is the most-studied nonmetal dopant for enhancing the visible light activity of  $\text{TiO}_2$  (Marschall and Wang, 2014).

There are several methods to produce N-doped TiO<sub>2</sub>, including hydrothermal, microemulsion, chemical vapor deposition, solvothermal, sol-gel, electrospinning, anodic oxidation, sputtering, ball milling, atomic layer deposition, and microwave (Basavarajappa et al., 2020). Several studies have produced N-doped TiO<sub>2</sub> for tetracyclines degradation under visible light (Wang et al., 2011; Chen and Liu, 2016; Tang et al., 2018; Farhadian et al., 2019; Wu et al., 2020). Wu et al. prepared N-doped TiO<sub>2</sub>-P25 by treating TiO<sub>2</sub>-P25 with NH<sub>3</sub> gas flow at 500°C, and applied the catalyst for tetracycline degradation under visible light ( $\lambda = 420$ ). This N-doped TiO<sub>2</sub>-P25 displayed higher visible light sensitivity and enhanced photocatalytic performance due to the increased numbers of excited reactive electrons and holes. The authors confirmed that the presence of N in TiO<sub>2</sub> created oxygen vacancies that entrapped the photoexcited electrons, thereby minimizing their recombination effect. The N-doped TiO<sub>2</sub>-P25 tetracycline degradation performance (90%) was higher than that of the unmodified TiO<sub>2</sub> (73%), and the doped photocatalyst maintained its stability and degradation efficiency for four consecutive cycles (Wu et al., 2020).

Carbon doping of Titania extends its light absorption into the visible region by acting as a sensitizer or by creating interstitial gap states in the catalyst structure (Palanivelu et al., 2007; Wu et al., 2013). Carbon doping also increases the number of photogenerated charge carriers that degrade organic pollutants in water (Palanivelu et al., 2007). Acetylene black-doped (AcB) and persulfate (PS)-employed TiO<sub>2</sub> (TiO<sub>2</sub>/AcB/PS) was prepared using the sol-gel method (Zhang T. et al., 2020). Acetylene black lowered the band gap energy of TiO<sub>2</sub> from 3.17 to 2.78 eV, thereby enabling it to be activated under visible light, efficiently minimizing charge carrier recombination, and promoting charge carrier separation. The TiO<sub>2</sub>/AcB/PS photocatalyst displayed (93%) tetracycline hydrochloride degradation efficiency, which was higher than that of unmodified TiO<sub>2</sub> (20%), and maintained high degradation efficiency (85%) after five uses (Zhang T. et al., 2020).

Phosphorus (P) doping of TiO<sub>2</sub> enhances the catalytic photoactivity by effectively suppressing charge carrier recombination due to electron entrapment by the oxygen vacancies created in the catalyst (Feng et al., 2018). The presence of a P dopant on TiO<sub>2</sub> decreased its band gap energy and significantly enhanced its visible light-induced photocatalytic degradation of organic pollutants (Gopal et al., 2012). Niu et al. (Niu et al., 2014) used the rapid microwave hydrothermal method to prepare P-doped anatase TiO<sub>2</sub> for tetracycline hydrochloride degradation under 500 W halogen-tungsten lamp. This P-doped TiO<sub>2</sub> displayed (93%) tetracycline degradation efficiency, which was much higher than that of commercial TiO<sub>2</sub>-P25 (62%).

Nonmetal element co-doping of TiO<sub>2</sub> has gained enormous interest lately because of its potential to alter the photocatalytic characteristics of the catalyst, such as reducing the band gap energy and enhancing visible light absorption as compared to that of the single-element-doped catalyst (Chen et al., 2007). Co-doping and tri-doping were applied to TiO<sub>2</sub> for enhanced tetracycline degradation. Wang

et al. (Wang et al., 2011) used the sol-gel method to prepare C-N-S tri-doped TiO<sub>2</sub> for tetracycline degradation under 6 W white visible light lamp. The C-N-S tri-doped TiO<sub>2</sub> exhibited enhanced degradation performance (95%) compared to that of unmodified TiO<sub>2</sub> (25%). The authors ascribed this improvement to the high surface area of the modified catalyst, the formation of a well-defined TiO<sub>2</sub> anatase phase, the red shift of the light absorption spectrum of TiO<sub>2</sub>, the enhanced visible light sensitivity because of the narrowed band gap energy of TiO<sub>2</sub>, and the existence of carbon behaving as photosensitizer of TiO<sub>2</sub>, which led to synergistic enhancement of tetracycline adsorption.

### 5.1.3 Mixed Metal-Nonmetal Doping of TiO<sub>2</sub>

Mixed metal-nonmetal doping enables optimization of the advantages and minimization of the disadvantages of each doping method. This hybrid method specifically enhances the catalyst photo-efficiency by broadening the photo-activated spectrum toward the visible range. The N-TiO<sub>2</sub> catalyst is most commonly used for tetracyclines degradation under visible light, along with other nonmetal-doped TiO<sub>2</sub> in mixed doping systems (Huo et al., 2016; Chen and Liu, 2017; Rimoldi et al., 2018; Chen Y. et al., 2019; Ghoreishian et al., 2020). Rimoldi et al. (Rimoldi et al., 2018) used the sol-gel method to prepare Sn-, Zn-, and N-doped TiO<sub>2</sub> for tetracycline degradation under simulated solar irradiation. The authors reported that metal co-doping of N-doped TiO<sub>2</sub> induced a further red-shift in the light spectrum (400–600 nm). They attributed this improvement to the generation of intra-gap states in the TiO<sub>2</sub> structure by the introduction of some defects caused by Sn-doping. TiO<sub>2</sub>-N was reported to have quasi-spherical crystallites of high crystallinity and corresponding inter-planar distances of anatase TiO<sub>2</sub>. For TiO<sub>2</sub>-N-Sn crystalline particles (3–6 nm) were detected along with the corresponding inter-planar distances of anatase and brookite TiO<sub>2</sub> and small content of SnO<sub>2</sub> cassiterite. In the TiO<sub>2</sub>-N-Zn, the presence of Zn resulted in the formation of a guest phase of ZnO wurtzite. Particularly, Zn doping resulted in better photocatalytic performance due to its low crystallinity, unique amorphous structure, and high surface area as compared to the Sn-doping alone. The mixed metal-nonmetal Zn/Sn/N-doped TiO<sub>2</sub> exhibited (33%) tetracycline degradation efficiency compared to (22%) tetracycline degradation efficiency of the unmodified TiO<sub>2</sub>. This significant increase was attributed to the synergistic effect of the dopants, their ability to widen the light absorption spectrum, and the higher surface area of the catalyst. Although (33%) tetracycline degradation efficiency is relatively low, the selected metal-nonmetal pairs and their concentrations can be optimized to improve photocatalyst performance.

In general, co- or tri-doping of TiO<sub>2</sub> can overcome some of the drawbacks of single doping, and enhance catalyst performance and stability in tetracyclines degradation due to the synergistic effect among the dopants. The choice of the dopant should consider its cost, toxicity, doping conditions, and preparation method. The dopant concentration also needs to be optimized to ensure enhanced performance of the final catalyst (Marschall and Wang, 2014).

**TABLE 6 |** Examples of titania-based composites and their tetracyclines degradation efficiencies.

#	Modified titania	Tetracycline initial concentration (mg/L)	Catalyst concentration	Light source	pH	Removal % by TiO <sub>2</sub> -Based composite catalysts	Removal % by unmodified TiO <sub>2</sub>	Year and ref
A. Immobilized titania composites								
1	Chitosan modified N-, S-doped TiO <sub>2</sub>	10 (TC)	0.6 g/L	Visible light <sup>a</sup>	8.2	92% after 50 min	–	2019 Farhadian et al. (2019)
2	2D sandwich-like TiO <sub>2</sub> -rGO composite	20 (TCH)	0.4 g/L	Xenon (Xe) lamp <sup>a</sup>	5.2	96% after 120 min	28% after 120 min	2017 Zhang S. et al. (2017)
3	Fe <sub>2</sub> O <sub>3</sub> -TiO <sub>2</sub> -modified zeolite composites	20 Oxy-(TC)	1 g/L	200 W λ = 455 nm LED light	Free	98% after 60 min	–	2019 Liu M. et al. (2019)
4	N-doped TiO <sub>2</sub> /rGO	10 (TCH)	1 g/L	300 W Xe lamp (λ > 400 nm)	7	98% after 60 min	10% after 60 min	2018 Tang et al. (2018)
5	Ce/N co-doped TiO <sub>2</sub> /NiFe <sub>2</sub> O <sub>4</sub> /diatomite	20 (TC)	0.5 g/L	150 W Xe lamp (λ > 400 nm)	7	100% after 180 min	–	2017 Chen and Liu, (2017)
6	Floating Fe/N co-doped TiO <sub>2</sub> /diatomite	10 (TC)	5 g/L	150 W Xe lamp (filter to isolate UV light) <sup>a</sup>	Free	96.5% after 150 min	–	2019 Chen Y. et al. (2019)
7	Zn-doped TiO <sub>2</sub> nanoparticles/GO	40 (TC)	1 g/L	500 W Xe lamp <sup>a</sup>	Free	98.5% after 120 min	20% after 120 min	2017 Zhang F. J. et al. (2017)
8	Cobalt-doped TiO <sub>2</sub> nanosheets/rGO	20 Oxy-(TCH)	1 g/L	500 W halogen lamp (350 < λ < 800 nm)	Free	68% after 180 min	–	2019 Jamali Alyani et al. (2019)
9	N-doped TiO <sub>2</sub> /diatomite	20 (TCH)	5 g/L	Xe lamp <sup>a</sup>	6	93% after 300 min	–	2016 Chen and Liu, (2016)
10	Black TiO <sub>2</sub> nanoparticle/porous carbon	50 (TC)	0.6 g/L	Xe lamp (λ > 420 nm)	5	90% after 160 min	–	2019 Fang et al. (2019)
11	Fe <sub>3</sub> O <sub>4</sub> /rGO/TiO <sub>2</sub> nanocomposites	20 (TCH)	0.4 g/L	150 W Xe lamp <sup>a</sup>	3	92.6% after 330 min in the presence of H <sub>2</sub> O <sub>2</sub>	–	2017 Wang W. et al. (2017)
12	Silver/TiO <sub>2</sub> nanosheets/rGO	30 (TC)	0.75 g/L	Halogen 500 W lamp (350 < λ < 800 nm)	7	52.56% after 180 min	–	2020 Tabatabai-Yazdi et al. (2020)
13	Ce-doped TiO <sub>2</sub> -MGO hybrid photocatalyst	25 (TC)	0.5 g/L	300 W Xe lamp <sup>a</sup>	Free	82.92% after 60 min	10.9% after 60 min	2016 Cao et al. (2016)
14	TiO <sub>2</sub> /Semnan natural zeolite	8 (TC)	0.8 g/L	60 W visible lamp <sup>a</sup>	6	87% after 90 min	10% after 90 min	2016 Saadati et al. (2016b)
15	Ce-doped TiO <sub>2</sub> /halloysite nanotubes	20 (TC)	0.5 g/L	300 W Xe lamp (λ > 420 nm)	7	78% after 60 min	8% after 60 min	2019 Wang et al. (2019)
16	Au-TiO <sub>2</sub> /polydopamine (pDA)-coated PVDF	10 (TC)	–	300 W Xe lamp (λ > 420 nm)	7	92% after 120 min	–	2017 Wang C. et al. (2017)
17	Bimetallic Au- and Ag-doped TiO <sub>2</sub> nanorods/cellulose acetate	5 (TC)	Fixed on a membrane	Xe lamp (λ > 420 nm)	Free	90% after 120 min	–	2019 Li W. et al. (2019)
18	C-doped titania-polymethylsilsesquioxane aerogels	10 (TCH)	10 g/L	Visible light (λ > 420 nm)	7	98% after 180 min	–	2021 Xu H. et al. (2021)
B. Nanostructured Titania Composites								
19	TiO <sub>2</sub> nanobelts modified by Au and CuS nanoparticles	5 Oxy-(TC)	4 cm <sup>2</sup>	Simulated solar light, a 35 W Xe lamp <sup>a</sup>	7	96% after 60 min	48% after 60 min by TiO <sub>2</sub> nanobelts	2016 Chen et al. (2016)
20	TiO <sub>2</sub> doped with acetylene black	10 (TCH)	0.5 g/L	30 W LED lamp (λ 400–780 nm)	4.1	93.3% after 120 min	20% after 120 min	2020 Zhang T. et al. (2020)
21	(1D) MIL-100(Fe)/TiO <sub>2</sub> nanoarrays	100 (TC)	Film sample	450 W Xe lamp <sup>a</sup>	Free	90.79% after 60 min	35.22% after 60 min	2018 He et al. (2018)
22	Ag/AgBr- modified TiO <sub>2</sub>	10 (TC)	1.2 g/L	5W LED white lamp <sup>a</sup>	4.5	95.3% after 60 min	20% after 60 min	2019 Sun et al. (2019)
23	TiO <sub>2</sub> -Fe <sub>2</sub> O <sub>3</sub>	15 (TC)	0.75 g/L	60 W lamp <sup>a</sup>	4.7	93% after 90 min	–	2019 Galedari et al. (2019)
24	Carbon-modified TiO <sub>2</sub>	5 (TCH)	0.3 g/L	White LED (λ = 450 nm)	7	73.53% after 120 min	40% after 120 min	2018 Oseghe and Ofomaja, (2018b)

(Continued on following page)

**TABLE 6 |** (Continued) Examples of titania-based composites and their tetracyclines degradation efficiencies.

#	Modified titania	Tetracycline initial concentration (mg/L)	Catalyst concentration	Light source	pH	Removal % by TiO <sub>2</sub> -Based composite catalysts	Removal % by unmodified TiO <sub>2</sub>	Year and ref
25	Pine cone-derived C-doped TiO <sub>2</sub>	5 (TCH)	0.3 g/L	25 W white vis-LED strip <sup>a</sup>	7	83% after 120 min	–	2018 Oseghe and Ofomaja, (2018a)
26	Bismuth-titanate nanoparticles	50 (TC)	1 g/L	360 W halogen lamp ( $\lambda > 400$ nm)	7	65% after 180 min	–	2017 Khodadoost et al. (2017)
27	C-TiO <sub>2</sub> nanocomposites	10 (TC)	0.2 g/L	–*	7	90% after 160 min	30% after 160 min	2019 Ma et al. (2019)
28	CdS-TiO <sub>2</sub> heterostructure composite	50 (TCH)	1 g/L	500 W Xe lamp ( $\lambda > 400$ nm)	7	87.06% after 480 min	7.68% after 480 min	2018 Li et al. (2018)
29	SrTiO <sub>3</sub> /Fe <sub>2</sub> O <sub>3</sub> nanowires	10 (TC)	1 g/L	250 W Xe lamp ( $\lambda > 420$ nm)	Free	82% after 140 min	–	2016 Liu et al. (2016)
30	Bi <sub>4</sub> Ti <sub>3</sub> O <sub>12</sub> /BiOCl composite	20 (TCH)	0.66 g/L	300W Xe lamp*	Free	83.7% after 150 min	–	2018 Liu et al. (2018)
31	Perovskite-type W-doped BaTiO <sub>3</sub>	5 (TC)	0.8 g/L	Visible metal halide light*	5.6	93% after 180 min	–	2019 Demircivi and Simsek, (2019)
32	Platinum-doped amorphous TiO <sub>2</sub> -filled mesoporous TiO <sub>2</sub>	50 (TCH)	0.5 g/L	500 W Xe lamp *	7	100% after 300 min	–	2019 Lyu et al. (2019)
33	Mn-doped SrTiO <sub>3</sub> nanocubes	10 (TC)	1 g/L	250 W Xe lamp ( $\lambda > 420$ nm)	7	66.7% after 60 min	–	2015 Wu et al. (2015)
34	Cu-doped TiO <sub>2</sub> micro/nanostructures	20 (TCH)	20 mg/L	1000 W Xe ( $\lambda > 420$ nm)	7	90% after 240 min by calcined Cu-doped TiO <sub>2</sub>	50% after 240 min	2018 Cao et al. (2018)
35	Carbon-doped TiO <sub>2</sub> ultrathin nanosheets	20 (TC)	0.5 g/L	300 W Xe lamp ( $\lambda > 420$ nm)	Free	89.1% after 120 min	50% after 120 min	2021 Bao et al. (2021)
36	rGO coordinated titania nanoplatelet	20 (TCH)	10 mg/L	500 W Xe lamp (350< $\lambda$ > 1,100 nm)	7	95% after 120 min	70% after 120 min	2020 Li C. et al. (2020)

<sup>a</sup>Light wavelength was not specified in the original paper.

Free pH: medium pH was not controlled.

Abbreviations: TC, tetracycline; TCH, tetracycline hydrochloride.

## 5.2 Titania-Based Composites

### 5.2.1 Immobilized Titania Composites

In addition to enhanced visible light activity, the practical and large scale application of Titania would necessitate catalyst stability and recyclability. Accordingly, many studies have investigated the immobilization of doped-TiO<sub>2</sub> on various polymeric (Chen Y. et al., 2019; Mahdavi et al., 2019), carbonaceous and ceramic supports such as polyphenylenediamine (POPD) (Yu et al., 2014), graphene, reduced graphene oxide (rGO) (Cao et al., 2016; Huo et al., 2016; Wang W. et al., 2017; Zhang F. J. et al., 2017; Tang et al., 2018; Jamali Alyani et al., 2019; Tabatabai-Yazdi et al., 2020), mesoporous carbon (Fang et al., 2019), MOFs (He et al., 2018; Yuan et al., 2021), zeolites (Saadati et al., 2016b; Liu M. et al., 2019), and silica (Yu et al., 2014; Chen and Liu, 2016; Chen and Liu, 2017; Zyoud et al., 2017; Li J. et al., 2019; Chen Y. et al., 2019; Wang et al., 2019). These systems are prepared as composites (Li R. et al., 2020), and the solid support provides three primary advantages: 1) high surface area which increases tetracycline adsorption, 2) enhanced light absorption and electron entrapment which enhances photocatalytic activity, and 3) reduced sintering and aggregation which leads to superior stability. The superior performance of these composite systems is also attributed to the presence of synergistic effects between the

dopant and support (Bahadar Khan and Kalsoom, 2019). **Table 6** presents examples of immobilized TiO<sub>2</sub>-based composite systems and their efficiencies for tetracycline degradation under visible light spectra.

Graphene is a planar form of carbon atoms with a crystal-like honeycomb structure, high specific surface area, good charge carrier transfer, zero band gap energy, and high interfacial adsorbing properties. Graphene immobilization of TiO<sub>2</sub> can shift the light spectrum absorbance of the photocatalyst toward visible light and minimize recombination of the electron/hole pairs (Koe et al., 2019). Zhang et al. (Zhang S. et al., 2017) prepared a 2D sandwich-like TiO<sub>2</sub>-reduced graphene oxide (TiO<sub>2</sub>-rGO) composite using the Pickering emulsion approach to investigate tetracycline hydrochloride degradation under xenon lamp as a visible light source. The unique mesoporous structure on both sides of the rGO significantly enhanced the tetracycline hydrochloride degradation by increasing the surface area of the catalyst and adsorption of the contaminant, promoting electron transfer, and minimizing recombination of the ( $e^-$ )/( $h^+$ ) pairs. TiO<sub>2</sub>-rGO degraded (96%) of the initial tetracycline hydrochloride concentration, whereas unmodified TiO<sub>2</sub> only degraded (28%) of the tetracycline hydrochloride. The authors suggested that the large number of mesoporous voids increased the number of exposed active sites of

TiO<sub>2</sub>, decreased the transport route length, and accelerated the electron transfer step. The visible light activity of this graphene-immobilized catalyst was attributed to the addition of rGO, which lowered the band gap energy of TiO<sub>2</sub> to 3.05.

Polymeric supports are nontoxic, low cost, widely available, resistant to UV light, durable, mechanically stable, and photo-stable. The hydrophobic properties of many polymers enables them to promote catalyst adsorption by increasing the pollutant concentration on its outer surface (Arif et al., 2020). Wang et al. (Wang C. et al., 2017) prepared a photocatalytic nanocomposite membrane of Au-doped TiO<sub>2</sub> supported on polydopamine (pDA)-coated polyvinylidene fluoride (PVDF) (Au-TiO<sub>2</sub>/pDA/PVDF). The nanocomposite membrane was used to degrade tetracycline under 300 W Xenon lamp as a visible light source. The authors reported that the visible light-induced tetracycline removal efficiency of Au-TiO<sub>2</sub>/pDA/PVDF was (51%) higher than that of undoped TiO<sub>2</sub>/pDA/PVDF and (26%) higher than that of Au-doped TiO<sub>2</sub>. They also reported that pDA acted as a glue to stabilize TiO<sub>2</sub> on the PVDF membrane, and functioned as a photosensitizer to widen the light absorbance spectrum of the catalyst. The authors proposed that the plasmon resonance effect of Au enhanced catalyst activity by accelerating photogenerated electron transfer from Au into the conduction band of the mother catalyst TiO<sub>2</sub>.

Ceramics have a large surface area, very good permeability, excellent strength, and high absorptivity (Mohd Adnan et al., 2018). Chen et al. (Chen and Liu, 2017) used the sol-gel method to prepare a magnetically recyclable Ce/N co-doped TiO<sub>2</sub>/NiFe<sub>2</sub>O<sub>4</sub>/diatomite ternary hybrid catalyst (CN-TND) for tetracycline degradation under 150 W xenon lamp as a visible light source. Each of the N and Ce dopants improved the photocatalyst surface properties and suppressed the formation of TiO<sub>2</sub> crystals. The authors observed that Ce/N co-doped TiO<sub>2</sub>/diatomite exhibited a slight redshift in its light absorption spectrum. CN-TND had slightly better tetracycline degradation efficiency (98%) than the N-doped TiO<sub>2</sub>/NiFe<sub>2</sub>O<sub>4</sub>/diatomite (95%) degradation efficiency due to the addition of Ce. The presence of ferrite (NiFe<sub>2</sub>O<sub>4</sub>) enhanced electron transfer and reduced charge carrier recombination. The improved performance of CN-TND was ascribed to the synergistic effect of the Ce and N dopants, which effectively widened the visible light absorption by the catalyst. CN-TND had ferromagnetism properties, was easily recovered from the reaction medium, and was reused five times with minimal loss in activity (0.5%). CN-TND achieved nearly complete tetracycline mineralization with (100%) TOC removal compared to only (52%) removal by the Ce/N co-doped TiO<sub>2</sub>.

Microporous structured supports such as zeolites were investigated for TiO<sub>2</sub> modification. Liu et al. (Liu M. et al., 2019) used the hydrothermal method to synthesize a Fe<sub>2</sub>O<sub>3</sub>-TiO<sub>2</sub>/Fe-Zeolite immobilized composite (Fe<sub>2</sub>O<sub>3</sub>-TiO<sub>2</sub>/FeZ). The composite catalyst was tested for oxytetracycline degradation using a 200 W 455 nm LED lamp as a visible light source. The Fe<sub>2</sub>O<sub>3</sub>-TiO<sub>2</sub>/FeZ composite exhibited a higher surface area (1,445 m<sup>2</sup>/g) than that of zeolite (844 m<sup>2</sup>/g), and had outstanding adsorption of oxytetracycline (94%) and improved activity under visible light. The visible light photocatalytic degradation efficiency of Fe<sub>2</sub>O<sub>3</sub>-TiO<sub>2</sub>/FeZ was (98%),

indicating its improved visible light absorption (400–600 nm), high adsorption of oxytetracycline, and enhanced rate of photogenerated charge carriers. Fe<sub>2</sub>O<sub>3</sub>-TiO<sub>2</sub>/FeZ had good stability after the fourth use and maintained (80%) efficiency.

In addition to zeolites, metal-organic frameworks (MOFs) have been investigated for the immobilization of TiO<sub>2</sub>. MOFs are hybrid organic-inorganic, low cost, and environmentally friendly micro-porous materials with unique morphological properties and superior surface areas (Gautam et al., 2020). When combined with semiconductors such as TiO<sub>2</sub>, MOFs form hierarchical nanostructures with enhanced photocatalytic properties (He et al., 2018). He et al. (He et al., 2018) applied one-dimensional MOF [Materials Institute Lavoisier 1D (MIL)-100(Fe)] over TiO<sub>2</sub> nanoarrays [1D MIL-100(Fe)/TiO<sub>2</sub>] by insitu growth of MIL-100(Fe) on the TiO<sub>2</sub> nanoarrays. The catalyst was tested for tetracycline degradation using a 450 W Xe lamp as a visible light source (He et al., 2018). The growth of 1D MIL-100(Fe) over TiO<sub>2</sub> nanoarrays increased the surface roughness of these nanoarrays, enhanced the visible light absorption of the composite catalyst (<600 nm), and improved the electron/hole separation and the accessibility of active sites. The composite 1D MIL-100(Fe)/TiO<sub>2</sub> photocatalyst achieved (90.79%) tetracycline degradation efficiency compared to only (35.22%) degradation efficiency achieved by unmodified TiO<sub>2</sub> nanoarrays. The composite catalyst was easily recovered and maintained good stability (70%) after the fifth use.

The proposed mechanism of tetracycline degradation by 1D MIL-100(Fe)/TiO<sub>2</sub> is presented in **Figure 4**. Upon irradiation, electrons in the VB of TiO<sub>2</sub> are excited into its CB (**Eq. 1**), while MIL-100(Fe) is activated *via* the direct excitation of FeO as well as ligand-to-metal charge transfer. The electrons and holes react with water and oxygen molecules to produce (•OH) and (O<sub>2</sub><sup>•-</sup>) radicals (**Eqs 2, 3, 7, 8, 9, 10**). In the presence of H<sub>2</sub>O<sub>2</sub>, Fe(III) in MIL-100(Fe) undergoes Fenton-like reactions and reacts with H<sub>2</sub>O<sub>2</sub> to further boost the formation of (•OH) radicals as shown in (**Figure 4**). The formed radicals synergistically degrade TC molecules under visible light (**Eqs 4, 5, 6**).

### 5.2.2 Nanostructured Titania Composites

Nanostructured Titania composites enhance the catalyst's surface area and crystal morphology, and they include TiO<sub>2</sub>-based nanospheres, nanosheets, nanowires, nanorods, nanotubes, and nanoparticles (Choi et al., 2014; Bahadar Khan and Kalsoom, 2019). Nanostructured Titania composites also enhance chemical, mechanical, electronic, and optical properties of Titania. **Table 6** presents examples of nanostructured TiO<sub>2</sub>-based composite systems that have been used for tetracyclines degradation under visible light.

Chen et al. (Chen et al., 2016) used the electrochemical anodic oxidation method to modify immobilized TiO<sub>2</sub> nanobelts (NBs) with Au and CuS nanoparticles, and tested the composite catalyst for oxytetracycline removal using simulated solar light irradiation (35 W Xe lamp). Au-CuS/TiO<sub>2</sub> NBs exhibited enhanced visible light (solar) absorption due the lowest band gap energy (2.65 eV) and the highest visible light absorption intensity (520–620 nm) compared to Au-TiO<sub>2</sub> NBs, CuS-TiO<sub>2</sub> NBs, and TiO<sub>2</sub> NBs. The oxytetracycline degradation efficiency of Au-CuS/TiO<sub>2</sub> NBs after

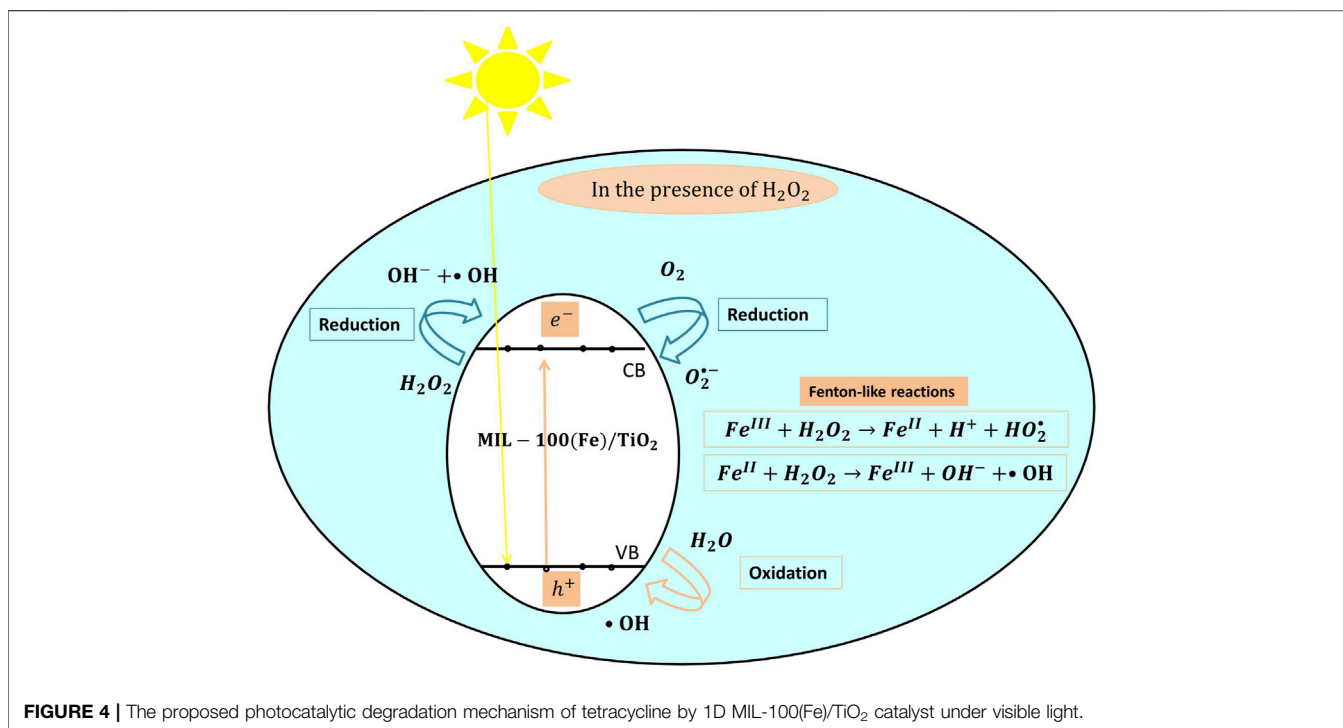


**FIGURE 4** | The proposed photocatalytic degradation mechanism of tetracycline by 1D MIL-100(Fe)/TiO<sub>2</sub> catalyst under visible light.

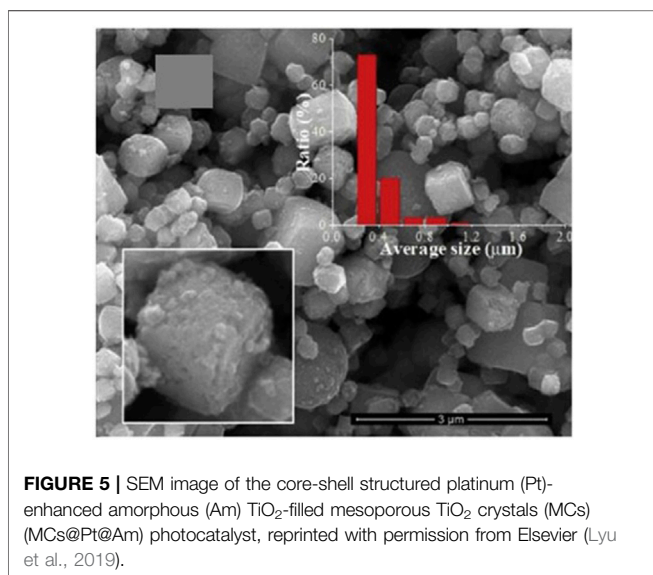


**FIGURE 5** | SEM image of the core-shell structured platinum (Pt)-enhanced amorphous (Am) TiO<sub>2</sub>-filled mesoporous TiO<sub>2</sub> crystals (MCs) (MCs@Pt@Am) photocatalyst, reprinted with permission from Elsevier (Lyu et al., 2019).

1 h was as high as (96%), whereas the oxytetracycline degradation efficiencies of Au-TiO<sub>2</sub> NBs, CuS-TiO<sub>2</sub> NBs, and TiO<sub>2</sub> NBs were (85%), (76%), and (66%), respectively. The authors ascribed the improved degradation efficiency of this catalyst to its ability to hinder recombination of photogenerated electron-hole pairs as a result of efficient interfacial charge transfer, and to the increased number of charge carriers participating in photocatalysis. The authors also concluded that visible light absorption was promoted by the plasmon resonance effect of Au, whereas CuS-TiO<sub>2</sub> NBs promoted

light absorption in the near-infrared region. Additionally, the authors attributed the improved performance of Au-CuS/TiO<sub>2</sub> to the ideal dispersion of both the Au and CuS on the smooth surface of TiO<sub>2</sub> NBs that formed a uniform surface composite structure. The total organic carbon (TOC) removal efficiency achieved by Au-CuS/TiO<sub>2</sub> NBs was (68%), whereas that of TiO<sub>2</sub> NBs was only (40%).

Lyu et al. (Lyu et al., 2019) used the hydrothermal method coupled with chemical reduction to prepare platinum (Pt)-enhanced amorphous (Am) TiO<sub>2</sub>-filled mesoporous TiO<sub>2</sub> crystals (MCs) (MCs@Pt@Am). This catalyst was tested for tetracycline hydrochloride degradation using a 500 W xenon lamp as a visible light source (Lyu et al., 2019). The authors created a new hierarchical porous core-shell structure by filling amorphous TiO<sub>2</sub> in the pores of Pt-doped mesoporous TiO<sub>2</sub> crystals, and reported that the core-shell structured catalyst (**Figure 5**) exhibited a larger surface area and particle size, higher tetracycline hydrochloride adsorption capacity, and reduced shell thickness as compared to TiO<sub>2</sub> crystals. These properties inhibited recombination of the electron/hole pairs and facilitated the migration of the positive hole into the catalyst surface while Pt-doping reduced the band gap energy of the catalyst and enhanced its visible light absorption. The photocatalytic degradation efficiency of tetracycline hydrochloride by MCs@Pt@Am was (100%), whereas that of amorphous TiO<sub>2</sub>-coated mesoporous TiO<sub>2</sub> crystals was (89%), and that of mesoporous TiO<sub>2</sub> crystals was (60%). MCs@Pt@Am degraded (77%) of the initial TOC content, whereas amorphous TiO<sub>2</sub>-coated mesoporous TiO<sub>2</sub> crystals degraded only (60%) of the initial TOC concentration.

**TABLE 7** | Examples of titania-based heterojunction photocatalysts.

#	Modified titania	TCs initial concentration (mg/L)	Catalyst concentration	Light source	pH	Removal % by TiO <sub>2</sub> -Based heterojunction photocatalysts	Removal % by titania	Year and ref
A. Titania-Based heterojunctions: Binary heterojunctions								
1	TiO <sub>2</sub> @ sulfur- doped carbon nitride nanocomposite	10 (TC)	0.1 g/L	300 W xenon (xe) lamp ( $\lambda > 420$ nm)	4.5	98.1% after 60 min	35.1% after 60 min	2021 Divakaran et al. (2021)
2	N-doped TiO <sub>2</sub> @ Bi <sub>2</sub> W <sub>2</sub> Mo <sub>1-x</sub> O <sub>6</sub> core-shell nanofibers	40 (TC)	0.3 g/L	300 W Xe lamp ( $\lambda > 400$ nm)	6	100% after 90 min	20% after 90 min	2020 Ghoreishian et al. (2020)
3	TiO <sub>2</sub> nanoparticle/ SnNb <sub>2</sub> O <sub>6</sub> nanosheet	35 (TCH)	1 g/L	500 W Tungsten lamp <sup>a</sup>	Free	75.5% after 240 min	63.8% after 240 min	2017 Jin et al. (2017)
4	CuO/Ti-MCM-48	19.24 (TCH)	1 g/L	Solar simulator <sup>a</sup>	Free	93% after 80 min	50% after 80 min	2018 Duan et al. (2018)
5	TiO <sub>2</sub> -coated $\alpha$ -Fe <sub>2</sub> O <sub>3</sub> core-shell heterojunction	50 (TCH)	0.2 g/L	300 W Xe lamp ( $\lambda > 420$ nm)	5.5	100% after 120 min	–	2018 Zheng et al. (2018)
6	CeO <sub>x</sub> -coupled MIL-125-derived C-TiO <sub>2</sub>	40 (TC)	1 g/L	500 W Xe lamp ( $\lambda > 400$ nm)	Free	83.5% after 180 min	30.3% after 180 min	2021 Yuan et al. (2021)
7	Ultrafine TiO <sub>2</sub> nanoparticle-modified g-C <sub>3</sub> N <sub>4</sub> heterojunction	20 (TCH)	0.25 g/L	150 W Xe lamp <sup>a</sup>	7	99.4% after 120 min	95.81% after 120 min	2020 Zhang B. et al. (2020)
8	Black-TiO <sub>2</sub> /CoTiO <sub>3</sub> Z-scheme heterojunction	20 (TC)	1 g/L	50 W LED lamps (450< $\lambda$ < 650 nm)	Free	82.4% after 30 min	28.3% after 80 min by black-TiO <sub>2</sub>	2021 Mousavi and Ghasemi, (2021)
9	TiO <sub>2</sub> /high-crystalline g-C <sub>3</sub> N <sub>4</sub> composite	10 (TC)	0.2 g/L	300 W Xe lamp ( $\lambda > 400$ nm)	Free	91% after 120 min	6% after 120 min	2020 Guo et al. (2020)
10	Ag/Ag <sub>3</sub> PO <sub>4</sub> nanoparticles/ cobalt- doped TiO <sub>2</sub> nanosheets	20 (TC)	1 g/L	500 W halogen lamp <sup>a</sup>	Free	66.80% after 140 min	–	2021 Mokhtari Nesfchi et al. (2021)
11	TiO <sub>2</sub> -coupled NiTiO <sub>3</sub> nanocomposites	–	1 g/L	250 W Xe lamp (UV-vis, 300< $\lambda$ < 800 nm)	Free	58% after 120 min	–	2018 Lakhera et al. (2018)
12	BiOXs/TiO <sub>2</sub>	30 (TC)	0.2 g/L	300 W Xe lamp ( $\lambda > 400$ nm)	Free	90% after 180 min	80% after 180 min	2019 Li L. et al. (2019)
13	BiFeO <sub>3</sub> /TiO <sub>2</sub> p-n heterojunction	20 (TC)	1 g/L	300 W Xe lamp <sup>a</sup>	5	72.2% after 180 min	38.3% after 180 min	2021 Liao et al. (2021)
14	Co <sub>3</sub> O <sub>4</sub> -TiO <sub>2</sub> /GO	10 Oxy-(TC)	0.25 g/L	300 W Xe solar simulator ( $\lambda > 420$ nm)	Free	91% after 90 min	30% after 90 min	2017 Jo et al. (2017)
15	Reduced graphene oxide-Ag <sub>2</sub> O/TiO <sub>2</sub> nanobelts composites	10 (TC)	0.4 g/L	300 W Xe arc lamp ( $\lambda > 420$ nm)	Free	18% after 60 min	18% after 60 min	2017 Hu et al. (2017)
16	Z-scheme CdTe/TiO <sub>2</sub> heterostructure	20 (TCH)	0.6 g/L	400 W halogen lamp ( $\lambda > 420$ nm)	Free	78% after 30 min	62% after 30 min	2018 Gong et al. (2018)
17	Carbon fiber/TiO <sub>2</sub> /Bi <sub>2</sub> WO <sub>6</sub> heterojunctions	10 (TCH)	Bundles (length ~4 cm, weight 0.15 g)	300 W Xe lamp ( $\lambda > 400$ nm)	Free	95.1% after 60 min	–	2018 Xu et al. (2018)
18	TiO <sub>2</sub> /BiOCl composite	30 (TC)	1 g/L	300 W Xe lamp ( $\lambda > 400$ nm)	3	90% after 240 min	33% after 240 min	2019 Hu et al. (2019)
19	Mo-C co-doped TiO <sub>2</sub> with fluorine-doped tin- oxide	20 (TC)	–	500 W Xe lamp ( $\lambda > 420$ nm)	7	90% after 100 min	–	2019 Niu et al. (2019)
20	N-doped TiO <sub>2</sub> /calcium ferrite/diatomite	10 (TC)	1 g/L	150 W Xe lamp ( $\lambda > 400$ nm)	Free	91.7% after 120 min	–	2019 Chen Y. et al. (2019)
21	N-doped TiO <sub>2</sub> /strontium ferrite/diatomite	10 (TC)	2 g/L	150 W Xe lamp ( $\lambda > 400$ nm)	Free	92.2% after 120 min	–	2019 Wu, (2019)
22	g-C <sub>3</sub> N <sub>4</sub> @Co-TiO <sub>2</sub> membrane	20 (TCH)	5 mg of membranes (2 × 2 cm <sup>2</sup> )/10 ml of solution	300 W Xe lamp ( $\lambda > 420$ nm)	7	90.8% within 60 min	–	2020 Song et al. (2020)
23	CeO <sub>2</sub> /TiO <sub>2</sub> composites	40 (TC)	1 g/L	500 W Xe lamp ( $\lambda > 420$ nm)	Free	99% within 80 min	10% within 80 min	2020 Pudukudy et al. (2020)
24	MnCo <sub>2</sub> O <sub>4.5</sub> Deposited TiO <sub>2</sub> Nanotube Array	10 (TC)	2.25 cm <sup>2</sup>	500 W Xe lamp <sup>a</sup>	Free	93.1% within 120 min	–	2020 Bi et al. (2020)

(Continued on following page)

**TABLE 7 |** (Continued) Examples of titania-based heterojunction photocatalysts.

#	Modified titania	TCs initial concentration (mg/L)	Catalyst concentration	Light source	pH	Removal % by TiO <sub>2</sub> -Based heterojunction photocatalysts	Removal % by titania	Year and ref
B. Titania-Based Heterojunctions: Ternary Heterojunctions								
25	Carbon plane/g-C <sub>3</sub> N <sub>4</sub> /TiO <sub>2</sub> nanocomposite	10 (TC)	1 g/L	500 W Xe lamp ( $\lambda$ > 400 nm)	Free	94.0% after 180 min	46% after 180 min	2019 Liu C. et al. (2019)
26	K-doped g-C <sub>3</sub> N <sub>4</sub> /TiO <sub>2</sub> /CdS	20 (TC)	1 g/L	300 W Xe lamp ( $\lambda$ > 420 nm)	Free	94.2% after 30 min	69.47% after 30 min	2021 Liu et al. (2021)
27	g-C <sub>3</sub> N <sub>4</sub> /Ti <sub>3</sub> C <sub>2</sub> /TiO <sub>2</sub> nanotube arrays on Ti meshes	10 (TCH)	1.5 × 1.0 cm	300 W Xe lamp ( $\lambda$ > 420 nm)	Free	85.12% after 180 min	—	2020 Diao et al. (2020)
C. Titania-Based Homogeneous Junctions: Facet Junction								
28	{101} and {001} facets co-exposed TiO <sub>2</sub> hollow sphere	10 (TC)	0.2 g/L	300 W Xe lamp ( $\lambda$ > 400 nm)	Free	90.1% after 120 min	—	2020 Zhang S. et al. (2020)

<sup>a</sup>Light wavelength was not specified in the original paper.

Free pH: medium pH was not controlled.

Abbreviations: TC, tetracycline; TCH, tetracycline hydrochloride.

All reported composite systems significantly improve TiO<sub>2</sub> catalyst performance for tetracyclines degradation under visible light. These properties arise from the synergistic effects between different moieties of the composite system and from the enhanced surface area and morphology of the photocatalyst. Many studies have successfully constructed and applied immobilized and nanostructured Titania composites for tetracycline degradation under visible light, and we conclude that both approaches are valuable for Titania modification. Although both immobilized and nanostructured Titania composites have high AB degradation efficiency percentages (>90%), immobilized Titania composites are preferred over nanostructured Titania composites due to their ease of recovery and reuse, especially in industrial applications.

### 5.3 Titania-Based Heterojunctions

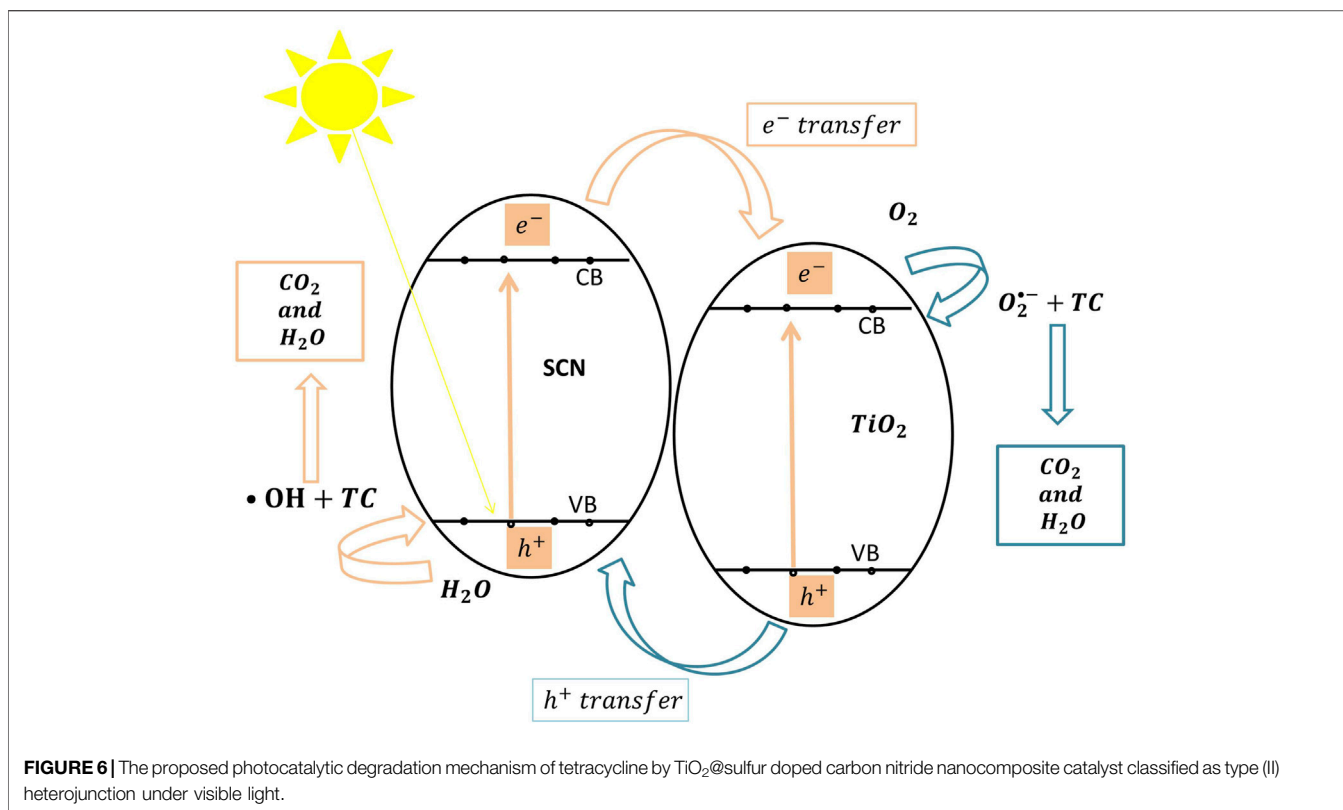
Heterojunction construction is another approach for the modification of Titania and the enhancement of its photocatalytic properties (Marcelino and Amorim, 2019; Li R. et al., 2020). Heterojunctions are constructed by forming a direct contact interface between two different semiconductors (Li R. et al., 2020; Yang et al., 2021). The two semiconductors must have different band gaps, a wide band gap (TiO<sub>2</sub>) and a narrow band gap, with the minimum band gap energy in the visible light region (Marcelino and Amorim, 2019; Li R. et al., 2020). This condition enhances the visible light absorption and photocatalytic activity of the heterojunction (Li R. et al., 2020). Heterojunctions promote the migration of charge carriers (electrons and holes) from one semiconductor to the other and minimize charge carrier recombination (Marcelino and Amorim, 2019; Li R. et al., 2020). Most TiO<sub>2</sub>-based heterojunctions are binary and can be classified based on the mechanism of separation of (e<sup>-</sup>)/(h<sup>+</sup>) pairs: p-n heterojunctions; type I (straddling gap); type II

(staggered gap); type III (broken gap); and direct Z-scheme heterojunctions (Li R. et al., 2020; Yang et al., 2021). **Table 7** summarizes these systems along with their efficiencies for tetracyclines degradation under various visible light irradiations. As shown in **Table 7**, binary heterojunctions are the most widely applied composites compared to ternary heterojunctions and homojunctions. Although ternary heterojunctions have very good tetracyclines removal efficiencies under visible light compared to binary heterojunctions, they require the use of an additional semiconductor, which involves additional costs.

#### 5.3.1 Binary TiO<sub>2</sub>-Based Heterojunctions

Binary heterojunctions are composed of two different semiconductors with different band gap energy levels (Marchelek et al., 2016). Conventional binary heterojunctions include type (I), type (II), and type (III) (Low et al., 2017). Nonconventional binary heterojunctions include p-n heterojunctions and Z-scheme heterojunctions (Li R. et al., 2020). The various conduction and valence level arrangements and mechanisms of these heterojunction catalysts are detailed in the following references (Low et al., 2017; Li R. et al., 2020).

Examples of binary TiO<sub>2</sub>-based heterojunctions include TiO<sub>2</sub>/BiOCl (Hu et al., 2019) and  $\alpha$ -Fe<sub>2</sub>O<sub>3</sub>@TiO<sub>2</sub> (Zheng et al., 2018). The  $\alpha$ -Fe<sub>2</sub>O<sub>3</sub>@TiO<sub>2</sub> is a type (I) heterojunction where the covalent bond (CB) of the first semiconductor (TiO<sub>2</sub>) exists at a higher position than the CB of the second semiconductor (Fe<sub>2</sub>O<sub>3</sub>), but the valence bond (VB) of Fe<sub>2</sub>O<sub>3</sub> is above that of TiO<sub>2</sub>. In this type, electrons move from the semiconductor with lower CB ( $\alpha$ -Fe<sub>2</sub>O<sub>3</sub>) into the semiconductor with higher CB (TiO<sub>2</sub>). The  $\alpha$ -Fe<sub>2</sub>O<sub>3</sub>@TiO<sub>2</sub> catalyst resulted in (100%) tetracycline hydrochloride degradation efficiency and (98%) TOC removal efficiency in



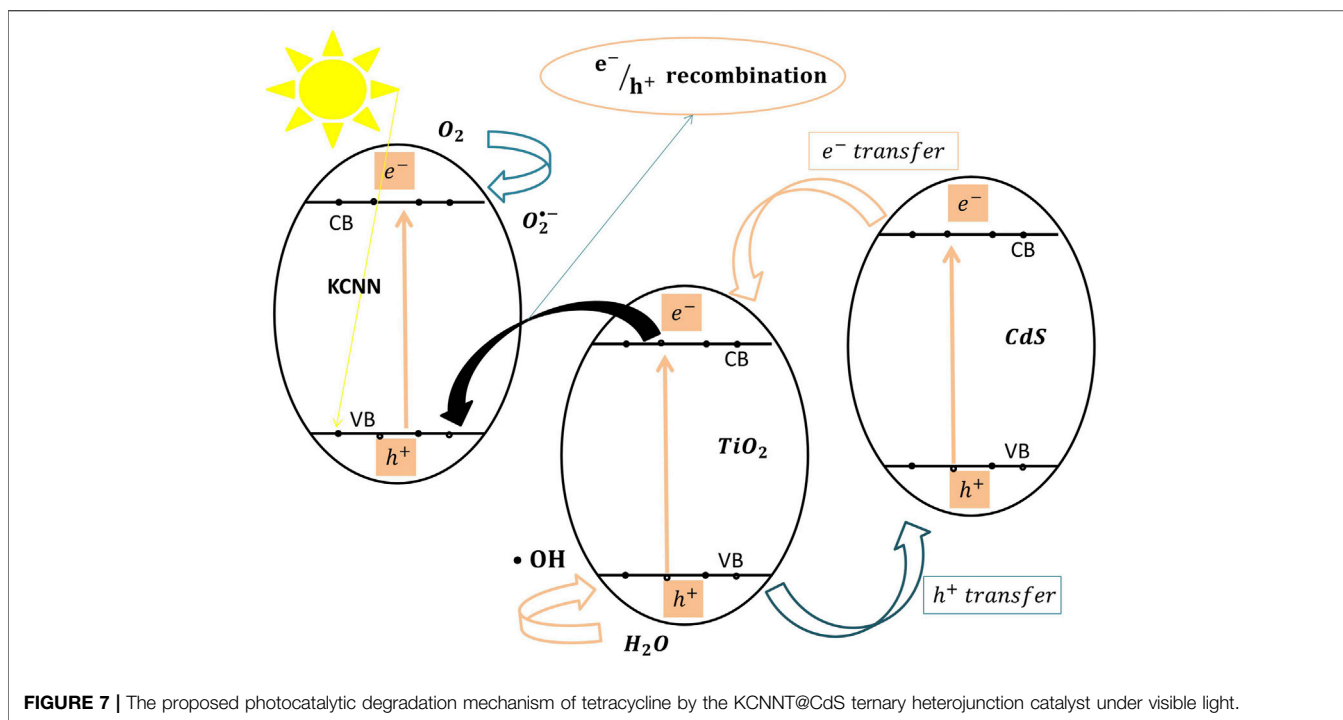
only 120 min using a 300 W xenon lamp (Zheng et al., 2018). The proposed mechanism for the degradation of tetracycline hydrochloride over the  $\text{Fe}_2\text{O}_3$ @ $\text{TiO}_2$  includes reduction/oxidation reactions by electron/hole pairs followed by the formation of the radicals (Eqs 2, 3, 7, 8, 9, 10) necessary for tetracycline hydrochloride degradation (Eqs 4, 5, 6).

The  $\text{TiO}_2$ -coated cubic  $\alpha$ - $\text{Fe}_2\text{O}_3$  core-shell heterojunction was synthesized using the hydrothermal method. The excellent visible light performance of the catalyst was primarily attributed to the well-matched interface between the cubic  $\alpha$ - $\text{Fe}_2\text{O}_3$  and  $\text{TiO}_2$  shell, the low band gap energy (1.97 eV), and enhanced visible light harvesting. The  $\alpha$ - $\text{Fe}_2\text{O}_3$ @ $\text{TiO}_2$  also had enhanced electron transfer through the heterojunction interface, better charge carrier separation, and minimized electron/hole recombination. The  $\alpha$ - $\text{Fe}_2\text{O}_3$ @ $\text{TiO}_2$  maintained excellent degradation efficiency (95%) and stability even after the fifth use. The authors reported that the core-shell structure of the  $\text{TiO}_2$  shell and the cubic morphology of  $\alpha$ - $\text{Fe}_2\text{O}_3$  core led to an enhanced electron transfer and minimized electron/hole recombination effect.

Several studies have investigated type (II)  $\text{TiO}_2$ -based binary heterojunctions.  $\text{TiO}_2$ @sulfur doped carbon nitride nanocomposite reported by Divakaran et al. (Divakaran et al., 2021) and  $\text{TiO}_2$ /SnNb $_2$ O $_6$  nanosheet reported by Jin et al. (Jin et al., 2017) are examples of this type of binary heterojunctions. In type (II), the CB and VB of the first semiconductor (sulfur doped carbon nitride: SCN) are higher than the corresponding CB and VB of the second semiconductor ( $\text{TiO}_2$ ) (Figure 6). This leads to significant

charge carrier separation because excited electrons migrate to the second semiconductor and the positive holes move into the first semiconductor.  $\text{TiO}_2$ @sulfur doped carbon nitride nanocomposite achieved (98.1%) degradation efficiency of the initial tetracycline concentration in 60 min, and the  $\text{TiO}_2$ /SnNb $_2$ O $_6$  nanosheet achieved (75.5%) degradation efficiency of tetracycline hydrochloride. Additionally, Gong et al. (Gong et al., 2018) applied Z-scheme CdTe/ $\text{TiO}_2$  heterojunction which was able to degrade (78%) of the initial tetracycline hydrochloride concentration after 30 min. A Z-scheme heterojunction has the same CB and VB arrangements of type (II) heterojunction with totally different electron migration route between the first and second semiconductors (Low et al., 2017; Li R. et al., 2020). Upon photo-excitation of electrons, the photo-generated electrons in the second semiconductor combine with the positive holes in the first semiconductor. Consequently, these electron/hole pairs generate the reactive radicals *via* (Eqs 2, 3, 7, 8, 9, 10) which themselves degrade the TC into  $\text{CO}_2$  and  $\text{H}_2\text{O}$  via (Eqs 4, 5, 6).

Liao et al. (Liao et al., 2021) prepared a binary p-n junction using BiFeO $_3$ / $\text{TiO}_2$  catalyst, and reported a (72.2%) tetracycline degradation efficiency after 180 min. This catalyst is composed of p-type and n-type semiconductors separated by a charged space region around the interface known as an internal electric field. This electric field minimizes charge carrier recombination by accelerating migration of the excited electrons and positive holes into the CB of the n-type semiconductor and VB of the p-type semiconductor, respectively (Low et al., 2017). In the mechanism



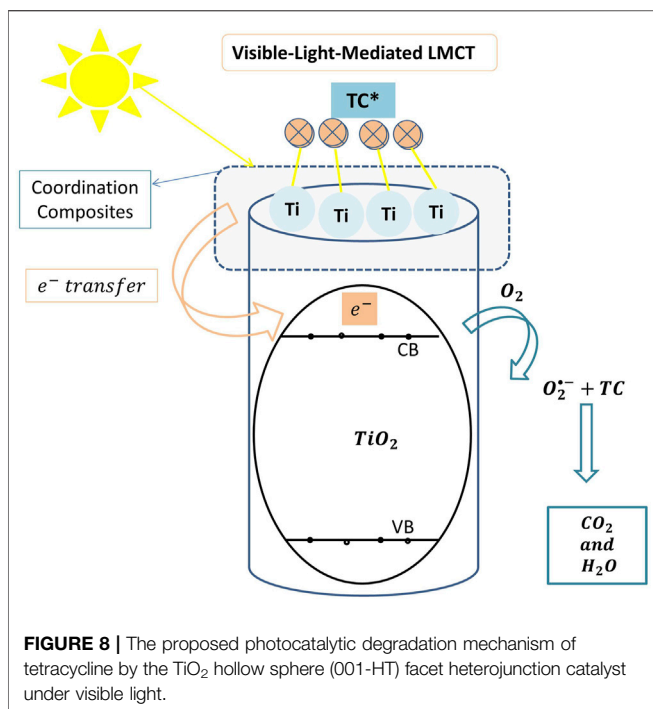
proposed by Liao et al., excited electrons in the CB of BiFeO<sub>3</sub> move into the CB of n-type TiO<sub>2</sub> semiconductor and similarly the positive holes in the VB of BiFeO<sub>3</sub> move into VB of n-type TiO<sub>2</sub> ensuring minimized recombination effect of ( $h^+$ )/( $e^-$ ). The rapid migration of the charge carriers in this catalyst is mainly due to the ferroelectric effect of BiFeO<sub>3</sub>. While ( $h^+$ ) oxidizes water molecules into hydroxyl radicals, ( $e^-$ ) reduces adsorbed oxygen molecules into super oxide radicals (Eqs 2, 3, 7, 8, 9, 10). Tetracycline molecules are photocatalytically degraded by these radicals under visible light according to (Eqs 4, 5, 6).

### 5.3.2 Ternary TiO<sub>2</sub>-Based Heterojunctions

Ternary heterojunctions are composed of three coupled semiconductors to form a ternary contact interface, which enhances electron excitation and photo-efficiency (Marchelek et al., 2016). Liu et al. (Liu et al., 2021) used the hydrothermal method to construct a novel ternary composite heterojunction with superior photocatalytic properties, which consisted of a synthesized K-doped g-C<sub>3</sub>N<sub>4</sub>/TiO<sub>2</sub>/CdS (KCNNT@CdS) ternary heterojunction nanocomposite. This nanocomposite photocatalyst was tested for tetracycline degradation efficiency under visible light using a 300 W xenon lamp. This photocatalyst showed excellent visible light-induced tetracycline degradation efficiency (94.2%) as compared to that of unmodified TiO<sub>2</sub> (69.47%). KCNNT@CdS degraded (40.1%) of the initial TOC concentration after 30 min. The authors attributed this performance enhancement to the presence of CdS, which behaved as an electron supplier and promoted charge carrier separation. The presence of TiO<sub>2</sub> itself was crucial to enhance the adsorption of tetracycline molecules on the surface of the composite KCNNT@CdS. The K dopant on the g-C<sub>3</sub>N<sub>4</sub> nanosheet enhanced visible light absorption, and the nanostructured morphology of g-C<sub>3</sub>N<sub>4</sub> minimized charge carrier

recombination and enhanced electron transfer (Liu et al., 2020). KCNNT@CdS maintained excellent stability after four uses. **Figure 7** shows the photocatalytic degradation mechanism of the KCNNT@CdS ternary heterojunction system. In this proposed mechanism, CdS behaves as an electron provider for TiO<sub>2</sub> because all excited electrons of CdS migrate into the CB of TiO<sub>2</sub> and then move into the VB of KCNNT to combine with the positive holes. Specifically ( $\bullet$ OH), ( $h^+$ ), and ( $O_2^{\bullet-}$ ), generated according to (Eqs 2, 3, 7, 8, 9, 10) are critical for tetracycline degradation under visible light irradiation.

Immobilized TiO<sub>2</sub>-based heterojunction systems offer easy catalyst recovery. Carbonaceous nanomaterials function as catalyst supports and can form a heterojunction with TiO<sub>2</sub> at the molecular level, thereby generating a ternary heterojunction. The nanocarbon material in the ternary heterojunction participates in the photocatalytic degradation process by controlling the electron transfer mechanism (Scaria et al., 2020). Liu et al. (Liu M. et al., 2019) prepared a ternary carbon plane/g-C<sub>3</sub>N<sub>4</sub>/TiO<sub>2</sub> nanocomposite heterojunction by anchoring the carbon plane into g-C<sub>3</sub>N<sub>4</sub> and then coupling it with TiO<sub>2</sub>, and they tested it for tetracycline degradation under visible light using a 500 W xenon lamp. The authors reported that the presence of the carbon plane was necessary to form the required ternary heterojunction contact in the prepared carbon plane/g-C<sub>3</sub>N<sub>4</sub>/TiO<sub>2</sub> nanostructured catalyst. The carbon plane/g-C<sub>3</sub>N<sub>4</sub>/TiO<sub>2</sub> photocatalyst degraded (94.0%) of the initial tetracycline concentration, whereas unmodified TiO<sub>2</sub> only degraded (46%) of the tetracycline. This improved visible light activity of the photocatalyst was ascribed to the heterojunction structure with effective ternary contact that enhanced charge carrier separation and transfer, and the inhibited charge carrier recombination.



### 5.3.3 TiO<sub>2</sub>-Based Homogenous Facet Junctions

Homogenous facet junctions are composed of different crystal planes of the same semiconductor in the same catalyst particle. The exposed surfaces generate a synergistic effect that enables local redox reactions and enhances charge separation and photoexcitation of the electrons (Yang et al., 2021). Zhang et al. (Zhang S. et al., 2020) prepared a homogeneous facet junction composed of {101} and {001} facets that were co-exposed to a TiO<sub>2</sub> hollow sphere (001-HT) facet heterojunction using a gentle sodium fluoride (NaF) treatment. This catalyst was used for tetracycline degradation under visible light using a 300 W xenon lamp. The reported tetracycline degradation efficiency of the 001-HT facet heterojunction photocatalyst (90.1%) was higher than that of the {101} facet-exposed TiO<sub>2</sub> hollow sphere (HT) that was obtained without NaF treatment (80%). The authors attributed the improved photocatalytic degradation of 001-HT to the formation of a {101}/{001} facet heterojunction, which enhanced visible light absorption, extended the life of excited electrons, increased charge carrier migration, and minimized charge carrier recombination. The enhanced visible light absorption of 001-HT was attributed to ligand-to-metal charge transfer (LMCT) due to the formation of coordination complexes between tetracycline molecules and Ti (IV) ions (Figure 8). Higher surface area, larger pore diameter, rougher surface, and bigger crystalline grains were reported for (001-HT) as compared to (HT). The photogenerated electrons in the highest occupied molecular orbital (HOMO) of the tetracycline antibiotic migrate into the CB of TiO<sub>2</sub> hollow sphere while no electron excitation occurs in TiO<sub>2</sub>. The transferred electrons reduce the oxygen molecules into super oxide radicals which attack the tetracycline

molecules in the aqueous medium and convert them into H<sub>2</sub>O and CO<sub>2</sub> (Eqs 4, 5, 6).

## 5.4 Recommendations on Most Promising TiO<sub>2</sub> Systems for Tetracyclines Degradation

In summary, all previous studies investigating Titania modifications clearly indicate that a combination of more than one modification method is crucial to achieve superior properties of photoactivity, stability, and ease of recovery for practical applications of the catalyst. For example, metal/nonmetal doping can enhance the visible light absorption of Titania; however, further immobilization of the doped TiO<sub>2</sub> through the formation of composite systems is essential to enhance catalyst morphology, photocatalytic properties, and stability. In metal/nonmetal doping, optimal dopant concentrations are recommended to prevent excess charge carriers, which can promote charge carrier recombination (Sponza and Koyuncuoglu, 2019; Zhang et al., 2019). The construction of heterojunction composites through the formation of a direct interface between Titania and another semiconductor enhances TiO<sub>2</sub> photocatalytic properties by improving the migration rate of charge carriers (i.e., both electron and positive holes) and minimizing their recombination. However, large-scale application of heterojunction photocatalysts is limited due to the complexity of fabrication, high cost, and low recycling efficiency (Li R. et al., 2020; Yang et al., 2021). A conclusion on the optimal modification method requires a complete understanding of the thermodynamics of the surface redox reactions and reaction mechanisms (Basavarajappa et al., 2020).

Based on our literature review, the best performing systems include 1) TiO<sub>2</sub> nanobelts modified with Au and CuS nanoparticles composite (Chen et al., 2016) which degraded (96%) of the initial oxytetracycline concentration in 60 min, indicating excellent degradation efficiency compared to other composites; 2) N-doped TiO<sub>2</sub>/rGO composites (Tang et al., 2018) that exhibited superior activity, with (98%) tetracycline hydrochloride degradation efficiency in 60 min due to N-doping and the addition of the rGO support; 3) Fe<sub>2</sub>O<sub>3</sub>-TiO<sub>2</sub>/modified zeolite composite (Liu M. et al., 2019), which also exhibited 98% oxytetracycline degradation in 60 min. We recommend the following TiO<sub>2</sub> modifications to be further considered in future studies for the photocatalytic degradation of TCs and antibiotics in irrigation water:

- Non-metal doping of Titania (C and N) to enhance its activity under visible light, to achieve high stability, and to avoid toxic metal leaching in case of metal doping (Sections 5.1.2, 5.2.2, 5.3.1) (Palanivelu et al., 2007; Teoh et al., 2012; Wu et al., 2013; Marschall and Wang, 2014; Chen and Liu, 2016; Oseghe and Ofomaja, 2018a; Zhang T. et al., 2020; Li C. et al., 2020; Ghoreishian et al., 2020; Wu et al., 2020).
- Metal doping of Titania or composite formation using non-toxic and ferromagnetic element such as iron to enhance its visible light performance and facilitate its recovery in large-scale applications by external magnets due to the acquired

ferromagnetic property (**Section 5.2.1**) (Cao et al., 2016; Wang W. et al., 2017; Chen and Liu, 2017).

- Immobilization of the doped Titania on non-toxic supports such as carbonaceous materials to minimize recovery and maintenance costs in commercial applications and improve degradation efficiency (**Sections 5.2.1, 5.3.2**) (Cao et al., 2016; Zhang S. et al., 2017; Zhang F. J. et al., 2017; Tang et al., 2018; Liu C. et al., 2019; Fang et al., 2019; Jamali Alyani et al., 2019; Koe et al., 2019; Scaria et al., 2020).

- Formation of doped-Titania nanostructured composites (nanosheets, nanowires, nanobelts) that enhances the catalyst's surface area and performance and facilitates its recovery and reuse in industrial scale systems (**Section 5.2.2**) (Choi et al., 2014; Chen et al., 2016; Bahadar Khan and Kalsoom, 2019; Lyu et al., 2019; Li C. et al., 2020).

- Optimization of the synthesis procedures and immobilization steps of the TiO<sub>2</sub> to ensure high and stable efficiency upon continuous reuse and to facilitate the recovery of the deactivated catalyst for proper and safe disposal (Sponza and Koyuncuoglu, 2019; Zhang et al., 2019; Scaria et al., 2020).

- Avoid the construction of complex and expensive heterojunction Titania photocatalysts of low recyclability, because this will create additional costs in large-scale systems and thus lower the overall cost efficiency of the proposed system (Li R. et al., 2020; Yang et al., 2021).

## 6 THE ENVIRONMENTAL IMPACT OF THE TiO<sub>2</sub> MODIFIED SYSTEMS

The environmental impact of the materials used in TiO<sub>2</sub> modification should be considered during the development of visible light-activated TiO<sub>2</sub> based photocatalysts. Safe materials with low toxicity and durable supports should be employed for catalyst immobilization to reduce the release of metals and generating secondary pollutants. These considerations will protect the environment and minimize the costs of system maintenance and catalyst recovery (Marcelino and Amorim, 2019; Li R. et al., 2020). Another important aspect is the leaching of any of these materials, used for TiO<sub>2</sub> modification, into the water medium and eventually into the environment. Usually researchers investigate catalyst recovery and reuse without presenting a study on the possibility of leaching of these materials (Yang et al., 2017). Nevertheless, and specifically in metal doping of TiO<sub>2</sub>, some researchers did present leaching studies. For example, Wang et al. studied the leaching of Fe ions from Fe<sub>3</sub>O<sub>4</sub>/rGO/TiO<sub>2</sub> when used for the degradation of tetracycline hydrochloride. The authors reported only 0.5 mg/L of Fe leaching into the solution, during the first cycle of catalyst use, which they concluded to be negligible. Moreover, after five cycles of use (Wang W. et al., 2017), the samples were characterized by XRD and FTIR and no structural changes were detected, confirming the textural and structural stability of the Fe<sub>3</sub>O<sub>4</sub>/rGO/TiO<sub>2</sub> catalyst. For the CeO<sub>2</sub>/TiO<sub>2</sub> binary heterojunction, Pudukudy et al. (Pudukudy et al., 2020) confirmed using FESEM elemental mapping, no Ce leaching after the 7<sup>th</sup> use of the catalyst. Similarly, Bi et al. reported that the

leached percentages of Mn and Co metals from MnCo<sub>2</sub>O<sub>4.5</sub>/TiO<sub>2</sub> catalyst were in the range (4–10%). However, it was concluded that leaching reduced the degradation efficiency of TC by only 2.9% after five runs (Bi et al., 2020).

In general, the stability of the catalyst and the leaching probability would very much depend on the water medium and the photocatalytic degradation conditions, such as the pH (Yang et al., 2017). Therefore, in real irrigation water media, it may be expected to have more pronounced leaching of the various used elements compared to laboratory distilled water media. In fact, immobilizing the catalyst on carbonaceous materials like graphene can help minimize metal leaching from titania catalysts (Scaria et al., 2020). Although, as mentioned in the above examples, metal leaching does not seem to be significant in photocatalysis, researchers should study and report the leaching of any of the catalyst's components during a photocatalytic degradation reaction using analytical techniques such as atomic absorbance spectroscopy and/or inductively coupled plasma (Marcelino and Amorim, 2019). In general, catalysts that may lead to leaching and further polluting and toxifying the water streams should be avoided, to prevent the need for a further water purification step (Bhadouria et al., 2020).

## 7 CONCLUSIONS AND FUTURE RESEARCH

There is clear evidence for antibiotic contamination of global ecosystems, water, and edible crops. The level of antibiotic contamination depends on the regional production and consumption of these pharmaceuticals. The use of wastewater in irrigation, animal manure, and biosolids in agriculture are important routes for the introduction of ABs into the ecosystem and edible crops. Current technologies for removing/degrading these pharmaceuticals from wastewater, such as conventional methods (biological processes, coagulation, flocculation, sedimentation, and filtration) and membrane methods, are incapable of removing these low-level and persistent organic pollutants from water. The development of innovative and efficient removal/degradation methods is urgently needed. Photocatalytic degradation is a promising method for removing organic pollutants from wastewater before using it for crop irrigation. This review summarized the current knowledge of Titania modification for the photocatalytic removal/degradation of tetracyclines from water. Titania is the most promising and studied semiconductor in this technology due to its low cost, high stability, low toxicity, good activity, and ease of modification (Teoh et al., 2012; Ibhaddon and Fitzpatrick, 2013; Koe et al., 2019; You et al., 2019; Zhang et al., 2019). We recommend that a combination of methods is essential to achieve superior catalytic properties of photoactivity, stability, and ease of recovery; these methods include metal-nonmetal doping, construction of a heterojunction interface with a second semiconductor, and immobilization on a stable porous support.

The large-scale application of the proposed visible light active Titania for irrigation water is plausible, however, there still

remain many challenges to bring this into application. One of the primary challenges is that the efficiency of these photocatalytic systems in large scale applications remains limited due to various reasons. One of these is the low and non-uniform light transmission into the catalyst surface (Tong et al., 2012). This limitation can be overcome by optimizing the various components of the reaction medium including the photocatalyst, the light illumination, and the reactor design to develop a commercial system for irrigation water treatment (Li and Shi, 2016). Moreover, further research is required to enhance the activation of the photocatalyst over a wide range of wavelengths, including the visible light region. It is also necessary to improve the overall mineralization and quantum efficiencies and the ease of recyclability and reusability of these photocatalysts (Tong et al., 2012). A complete mineralization of the toxic organic compounds is essential to minimize the formation of byproducts, which in some cases could be more toxic than the initial pollutant (**Section 4.1**) (Calvete et al., 2019). Most of the studies discussed in this review lacked toxicity assessments of intermediate photoproducts. We recommend that researchers conduct toxicity studies along with studies of catalyst performance.

In addition, it is worth noting that most research on the modification of Titania and other semiconductors for AB degradation utilize laboratory-scale reactors containing synthetic solutions of antibiotics in distilled water rather than in real wastewater irrigation samples. However, the observed catalyst efficiency in these laboratory systems is an overestimate and does not reflect the real-world efficiency of the catalyst in contaminated water samples. Similarly, catalyst recovery in large-scale applications is expected to be more challenging than it is in small-scale laboratory experiments (Li R. et al., 2020).

To conclude, we recommend that further research is needed to bring Titania-based photocatalytic degradation of ABs into large scale application. An efficient and easily recyclable catalyst system should be coupled with an optimum reactor design and adequate light source to guarantee a feasible large scale application.

As for the impact on humans, we conclude that human consumption of AB-contaminated water and edible crops leads to health risks because it can potentiate antibiotic resistance in human pathogens. A clear assessment of the risks imposed by

antibiotic contaminants on human health is lacking. The ecotoxicological effects of using antibiotic-contaminated irrigation water and/or animal manure fertilizer have not been fully investigated and understood. This would require a clear understanding of the physiochemical properties of the antibiotics in the soil and the mechanisms of their translocation and bioaccumulation in plants (Pan and Chu, 2017). Field studies are required to accurately assess antibiotic uptake by various crops under different environmental conditions, and the impacts of antibiotic bioaccumulation in these plants (Pan and Chu, 2017).

Well-defined dietary studies are urgently needed to evaluate the impact of consumption of antibiotic-contaminated crops from real-world fields on human health (Pan and Chu, 2017). These studies should include participants of different ages consuming different edible crops planted in soil treated with different concentrations of animal manure and irrigated with antibiotic-containing wastewater.

## AUTHOR CONTRIBUTIONS

Conceptualization, CB; writing—original draft, GJ and IK; Review and editing, CB and AT; Supervision, CB; funding acquisition, CB and AT. All authors have read and agreed to the published version of the manuscript.

## FUNDING

Funding was provided by the WEFRAH (Water-Energy-Food-Health Nexus) initiative at the American University of Beirut (Project number: 25202, Award number: 103763).

## ACKNOWLEDGMENTS

The authors gratefully acknowledge the financial support provided by the WEFRAH initiative at the American University of Beirut. The authors greatly thank and acknowledge the scientific contribution of Prof. Isam Bashour, at the Faculty of Agriculture and Food Sciences at the American University of Beirut.

## REFERENCES

- Abi Khalil, P. F. (2008). *Quantification of Antibiotic Residue Levels and Determination of Antimicrobial Resistance Profiles of Microorganisms Isolated from Raw Milk in Lebanon*—by Pamela Fouad Abi Khalil in Dept. Of Nutrition and Food Science. Lebanon: American University of Beirut (AUB).
- Adams, C., Wang, Y., Loftin, K., and Meyer, M. (2002). Removal of Antibiotics from Surface and Distilled Water in Conventional Water Treatment Processes. *J. Environ. Eng.* 128 (3), 253–260. doi:10.1061/(asce)0733-9372(2002)128:3(253)
- Addamo, M., Augugliaro, V., Di Paola, A., García-López, E., Loddo, V., Marci, G., et al. (2005). Removal of Drugs in Aqueous Systems by Photoassisted Degradation. *J. Appl. Electrochemistry* 35 (7), 765–774. doi:10.1007/s10800-005-1630-y
- Akel, S., Boughaled, R., Dillert, R., El Azzouzi, M., and Bahnemann, D. W. (2020). UV/Vis Light Induced Degradation of Oxytetracycline Hydrochloride Mediated by Co-TiO<sub>2</sub> Nanoparticles. *Molecules* 25 (2), 249. doi:10.3390/molecules25020249
- Andreozzi, R., Canterino, M., Marotta, R., and Paxeus, N. (2005). Antibiotic Removal from Wastewaters: The Ozonation of Amoxicillin. *J. Hazard. Mater.* 122 (3), 243–250. doi:10.1016/j.jhazmat.2005.03.004
- Anjali, R., and Shanthakumar, S. (2019). Insights on the Current Status of Occurrence and Removal of Antibiotics in Wastewater by Advanced Oxidation Processes. *J. Environ. Manage.* 246, 51–62. doi:10.1016/j.jenvman.2019.05.090
- Arif, Z., Sethy, N. K., Kumari, L., Mishra, P. K., and Upadhyay, S. N. (2020). “Recent Advances in Functionalized Polymer-Based Composite Photocatalysts for Wastewater Treatment,” in *Nano-Materials as Photocatalysts for Degradation of Environmental Pollutants*. Editor P. Singh (Elsevier), 39–64. doi:10.1016/b978-0-12-818598-8.00003-1

- Arslan-Alaton, I., and Dogruel, S. (2004). Pre-treatment of Penicillin Formulation Effluent by Advanced Oxidation Processes. *J. Hazard. Mater.* 112 (1), 105–113. doi:10.1016/j.jhazmat.2004.04.009
- Aznan, D., Mortey, C., Darko, G., Weisser, J. J., Styryshave, B., and Abaidoo, R. C. (2016). Uptake of Antibiotics from Irrigation Water by Plants. *Chemosphere* 157, 107–114. doi:10.1016/j.chemosphere.2016.05.035
- Bahadar Khan, S., and Kalsoom, A. (2019). “Modified Titanium Dioxide for Photocatalytic Applications,” in *Photocatalysts - Applications and Attributes*.
- Bao, S., Liu, H., Liang, H., Li, C., and Bai, J. (2021). Electrospun Silk-ribbon-like Carbon-Doped TiO<sub>2</sub> Ultrathin Nanosheets for Enhanced Visible-Light Photocatalytic Activity. *Colloids Surf. A: Physicochemical Eng. Aspects* 616, 126289. doi:10.1016/j.colsurfa.2021.126289
- Basavarajappa, P. S., Patil, S. B., Ganganagappa, N., Reddy, K. R., Raghu, A. V., and Reddy, C. V. (2020). Recent Progress in Metal-Doped TiO<sub>2</sub>, Non-metal Doped/codoped TiO<sub>2</sub> and TiO<sub>2</sub> Nanostructured Hybrids for Enhanced Photocatalysis. *Int. J. Hydrogen Energ.* 45 (13), 7764–7778. doi:10.1016/j.ijhydene.2019.07.241
- Bautitz, I. R., and Nogueira, R. F. P. (2010). Photodegradation of Lincomycin and Diazepam in Sewage Treatment Plant Effluent by Photo-Fenton Process. *Catal. Today* 151 (1), 94–99. doi:10.1016/j.cattod.2010.02.018
- Bhadouria, R., Mishra, D., Singh, V. K., Singh, P., Srivastava, P., Tripathi, S., et al. (2020). “Nanocatalyst Types and Their Potential Impacts in Agroecosystems: An Overview,” in *Nano-Materials as Photocatalysts for Degradation of Environmental Pollutants*. Editor P. Singh (Elsevier), 323–344. doi:10.1016/b978-0-12-818598-8.00016-x
- Bi, Y., Li, J., Dong, C., Mu, W., and Han, X. (2020). Rational Construction of MnCo<sub>2</sub>O<sub>4</sub> Deposited TiO<sub>2</sub> Nanotube Array Heterostructures with Enhanced Photocatalytic Degradation of Tetracycline. *ChemPhotoChem* 4 (5), 366–372. doi:10.1002/cptc.201900283
- Bouafia-Chergui, S., Zemmouri, H., Chabani, M., and Bensmail, A. (2016). TiO<sub>2</sub>-photocatalyzed Degradation of Tetracycline: Kinetic Study, Adsorption Isotherms, Mineralization and Toxicity Reduction. *Desalination Water Treat.* 57 (35), 16670–16677. doi:10.1080/19443994.2015.1082507
- Calvete, M. J. F., Piccirillo, G., Vinagreiro, C. S., and Pereira, M. M. (2019). Hybrid Materials for Heterogeneous Photocatalytic Degradation of Antibiotics. *Coord. Chem. Rev.* 395, 63–85. doi:10.1016/j.ccr.2019.05.004
- Cao, M., Wang, P., Ao, Y., Wang, C., Hou, J., and Qian, J. (2016). Visible Light Activated Photocatalytic Degradation of Tetracycline by a Magnetically Separable Composite Photocatalyst: Graphene Oxide/magnetite/cerium-Doped Titania. *J. Colloid Interf. Sci.* 467, 129–139. doi:10.1016/j.jcis.2016.01.005
- Cao, X., Tao, J., Xiao, X., and Nan, J. (2018). Hydrothermal-assisted Synthesis of the Multi-Element-Doped TiO<sub>2</sub> Micro/nanostructures and Their Photocatalytic Reactivity for the Degradation of Tetracycline Hydrochloride under the Visible Light Irradiation. *J. Photochem. Photobiol. A: Chem.* 364, 202–207. doi:10.1016/j.jphotochem.2018.06.013
- Carlesio Jara, C., Fino, D., Specchia, V., Saracco, G., and Spinelli, P. (2007). Electrochemical Removal of Antibiotics from Wastewaters. *Appl. Catal. B: Environ.* 70 (1), 479–487. doi:10.1016/j.apcatb.2005.11.035
- Chen, D., Jiang, Z., Geng, J., Wang, Q., and Yang, D. (2007). Carbon and Nitrogen Co-doped TiO<sub>2</sub> with Enhanced Visible-Light Photocatalytic Activity. *Ind. Eng. Chem. Res.* 46 (9), 2741–2746. doi:10.1021/ie061491k
- Chen, F., Li, D., Luo, B., Chen, M., and Shi, W. (2017). Two-dimensional Heterojunction Photocatalysts Constructed by Graphite-like C<sub>3</sub>N<sub>4</sub> and Bi<sub>2</sub>WO<sub>6</sub> Nanosheets: Enhanced Photocatalytic Activities for Water Purification. *J. Alloys Compd.* 694, 193–200. doi:10.1016/j.jallcom.2016.09.326
- Chen, M., Zhu, M., Zhu, Y., Wang, D., Li, Z., Zeng, G., et al. (2019). Collision of Emerging and Traditional Methods for Antibiotics Removal: Taking Constructed Wetlands and Nanotechnology as an Example. *NanoImpact* 15, 100175. doi:10.1016/j.impact.2019.100175
- Chen, Q., Wu, S., and Xin, Y. (2016). Synthesis of Au-CuS-TiO<sub>2</sub> Nanobelts Photocatalyst for Efficient Photocatalytic Degradation of Antibiotic Oxytetracycline. *Chem. Eng. J.* 302, 377–387. doi:10.1016/j.cej.2016.05.076
- Chen, W.-R., and Huang, C.-H. (2010). Adsorption and Transformation of Tetracycline Antibiotics with Aluminum Oxide. *Chemosphere* 79 (8), 779–785. doi:10.1016/j.chemosphere.2010.03.020
- Chen, Y., and Liu, K. (2017). Fabrication of Magnetically Recyclable Ce/N Co-doped TiO<sub>2</sub>/NiFe<sub>2</sub>O<sub>4</sub>/diatomite Ternary Hybrid: Improved Photocatalytic Efficiency under Visible Light Irradiation. *J. Alloys Compd.* 697, 161–173. doi:10.1016/j.jallcom.2016.12.153
- Chen, Y., and Liu, K. (2016). Preparation and Characterization of Nitrogen-Doped TiO<sub>2</sub>/diatomite Integrated Photocatalytic Pellet for the Adsorption-Degradation of Tetracycline Hydrochloride Using Visible Light. *Chem. Eng. J.* 302, 682–696. doi:10.1016/j.cej.2016.05.108
- Chen, Y., Wu, Q., Liu, L., Wang, J., and Song, Y. (2019). The Fabrication of Floating Fe/N Co-doped Titania/diatomite Granule Catalyst with Enhanced Photocatalytic Efficiency under Visible Light Irradiation. *Adv. Powder Technol.* 30 (1), 126–135. doi:10.1016/j.apt.2018.10.014
- Chen, Y., Wu, Q., Wang, J., and Song, Y. (2019). Retracted: The Fabrication of Magnetic Recyclable Nitrogen-doped Titanium Dioxide/calcium Ferrite/diatomite Heterojunction Nanocomposite for Improved Visible-light-driven Degradation of Tetracycline. *J. Chem. Technol. Biotechnol.* 94 (8), 2702–2712. doi:10.1002/jctb.6082
- Choi, H., Zakersalehi, A., Al-Abed, S. R., Han, C., and Dionysiou, D. D. (2014). “Nanostructured Titanium Oxide Film- and Membrane-Based Photocatalysis for Water Treatment,” in *Nanotechnology Applications for Clean Water*. Editor A. Street Second Edition (Oxford: William Andrew Publishing), 123–132. doi:10.1016/b978-1-4557-3116-9.00008-1
- Choi, K.-J., Kim, S.-G., and Kim, S.-H. (2008). Removal of Antibiotics by Coagulation and Granular Activated Carbon Filtration. *J. Hazard. Mater.* 151 (1), 38–43. doi:10.1016/j.jhazmat.2007.05.059
- Choi, K. J., Son, H. J., and Kim, S. H. (2007). Ionic Treatment for Removal of Sulfonamide and Tetracycline Classes of Antibiotic. *Sci. Total Environ.* 387 (1–3), 247–256. doi:10.1016/j.scitotenv.2007.07.024
- Christou, A., Agüera, A., Bayona, J. M., Cytryn, E., Fotopoulos, V., Lambropoulou, D., et al. (2017). The Potential Implications of Reclaimed Wastewater Reuse for Irrigation on the Agricultural Environment: The Knowns and Unknowns of the Fate of Antibiotics and Antibiotic Resistant Bacteria and Resistance Genes - A Review. *Water Res.* 123, 448–467. doi:10.1016/j.watres.2017.07.004
- Daghrir, R., and Drogué, P. (2013). Tetracycline Antibiotics in the Environment: a Review. *Environ. Chem. Lett.* 11 (3), 209–227. doi:10.1007/s10311-013-0404-8
- Danner, M.-C., Robertson, A., Behrens, V., and Reiss, J. (2019). Antibiotic Pollution in Surface Fresh Waters: Occurrence and Effects. *Sci. Total Environ.* 664, 793–804. doi:10.1016/j.scitotenv.2019.01.406
- Demircivi, P., and Simsek, E. B. (2019). Visible-light-enhanced Photoactivity of Perovskite-type W-Doped BaTiO<sub>3</sub> Photocatalyst for Photodegradation of Tetracycline. *J. Alloys Compd.* 774, 795–802. doi:10.1016/j.jallcom.2018.09.354
- Deng, Y., Tang, L., Zeng, G., Feng, C., Dong, H., Wang, J., et al. (2017). Plasmonic Resonance Excited Dual Z-Scheme BiVO<sub>4</sub>/Ag/Cu<sub>2</sub>O Nanocomposite: Synthesis and Mechanism for Enhanced Photocatalytic Performance in Recalcitrant Antibiotic Degradation. *Environ. Sci. Nano* 4 (7), 1494–1511. doi:10.1039/c7en00237h
- Di, J., Xia, J., Ge, Y., Li, H., Ji, H., Xu, H., et al. (2015). Novel Visible-Light-Driven CQDs/Bi<sub>2</sub>WO<sub>6</sub> Hybrid Materials with Enhanced Photocatalytic Activity toward Organic Pollutants Degradation and Mechanism Insight. *Appl. Catal. B: Environ.* 168–169, 51–61. doi:10.1016/j.apcatb.2014.11.057
- Diao, Y., Yan, M., Li, X., Zhou, C., Peng, B., Chen, H., et al. (2020). In-situ Grown of G-C<sub>3</sub>N<sub>4</sub>/Ti<sub>3</sub>C<sub>2</sub>/TiO<sub>2</sub> Nanotube Arrays on Ti Meshes for Efficient Degradation of Organic Pollutants under Visible Light Irradiation. *Colloids Surf. A: Physicochemical Eng. Aspects* 594, 124511. doi:10.1016/j.colsurfa.2020.124511
- Divakaran, K., Baishnisha, A., Balakumar, V., Perumal, K. N., Meenakshi, C., and Kannan, R. S. (2021). Photocatalytic Degradation of Tetracycline under Visible Light Using TiO<sub>2</sub>@sulfur Doped Carbon Nitride Nanocomposite Synthesized via In-Situ Method. *J. Environ. Chem. Eng.* 9 (4), 105560. doi:10.1016/j.jece.2021.105560
- Duan, Y., Zhai, D., Zhang, X., Zheng, J., and Li, C. (2018). Synthesis of CuO/Ti-MCM-48 Photocatalyst for the Degradation of Organic Pollutants under Solar-Simulated Irradiation. *Catal. Lett.* 148 (1), 51–61. doi:10.1007/s10562-017-2258-3
- Fang, Y., Li, Y., Zhou, F., Gu, P., Liu, J., Chen, D., et al. (2019). An Efficient Photocatalyst Based on Black TiO<sub>2</sub> Nanoparticles and Porous Carbon with High Surface Area: Degradation of Antibiotics and Organic Pollutants in Water. *ChemPlusChem* 84 (5), 474–480. doi:10.1002/cplu.201900103
- Farhadan, N., Akbarzadeh, R., Pirsahab, M., Jen, T.-C., Fakhri, Y., and Asadi, A. (2019). Chitosan Modified N, S-Doped TiO<sub>2</sub> and N, S-Doped ZnO for Visible Light Photocatalytic Degradation of Tetracycline. *Int. J. Biol. Macromolecules* 132, 360–373. doi:10.1016/j.jbiomac.2019.03.217

- Fazilati, M., Nozhat, S., and Borghei, S. M. (2018). "Comparing the Efficiency of TiO<sub>2</sub>/ZnO Catalysts in the Removal of Tetracycline from Aqueous Solution," in International Congress on Engineering Science and Sustainable Urban Development, Denmark – Copenhagen.
- Feng, X., Wang, P., Hou, J., Qian, J., Ao, Y., and Wang, C. (2018). Significantly Enhanced Visible Light Photocatalytic Efficiency of Phosphorus Doped TiO<sub>2</sub> with Surface Oxygen Vacancies for Ciprofloxacin Degradation: Synergistic Effect and Intermediates Analysis. *J. Hazard. Mater.* 351, 196–205. doi:10.1016/j.jhazmat.2018.03.013
- Galedari, M., Mehdipour Ghazi, M., and Rashid Mirmasoomi, S. (2019). Photocatalytic Process for the Tetracycline Removal under Visible Light: Presenting a Degradation Model and Optimization Using Response Surface Methodology (RSM). *Chem. Eng. Res. Des.* 145, 323–333. doi:10.1016/j.cherd.2019.03.031
- Gautam, S., Agrawal, H., Thakur, M., Akbari, A., Sharda, H., Kaur, R., et al. (2020). Metal Oxides and Metal Organic Frameworks for the Photocatalytic Degradation: A Review. *J. Environ. Chem. Eng.* 8, 103726. doi:10.1016/j.jece.2020.103726
- Ghoreishian, S. M., Ranjith, K. S., Lee, H., Ju, H.-i., Zeinali Nikoo, S., Han, Y.-K., et al. (2020). Hierarchical N-Doped TiO<sub>2</sub>@Bi<sub>2</sub>WxMo<sub>1-x</sub>O<sub>6</sub> Core-Shell Nanofibers for Boosting Visible-Light-Driven Photocatalytic and Photoelectrochemical Activities. *J. Hazard. Mater.* 391, 122249. doi:10.1016/j.jhazmat.2020.122249
- Ghoreishian, S. M., Ranjith, K. S., Lee, H., Park, B., Norouzi, M., Nikoo, S. Z., et al. (2021). Tuning the Phase Composition of 1D TiO<sub>2</sub> by Fe/Sn Co-doping Strategy for Enhanced Visible-Light-Driven Photocatalytic and Photoelectrochemical Performances. *J. Alloys Compd.* 851, 156826. doi:10.1016/j.jallcom.2020.156826
- Göbel, A., McArdell, C. S., Joss, A., Siegrist, H., and Giger, W. (2007). Fate of Sulfonamides, Macrolides, and Trimethoprim in Different Wastewater Treatment Technologies. *Sci. Total Environ.* 372 (2), 361–371. doi:10.1016/j.scitotenv.2006.07.039
- Gong, Y., Wu, Y., Xu, Y., Li, L., Li, C., Liu, X., et al. (2018). All-solid-state Z-Scheme CdTe/TiO<sub>2</sub> Heterostructure Photocatalysts with Enhanced Visible-Light Photocatalytic Degradation of Antibiotic Waste Water. *Chem. Eng. J.* 350, 257–267. doi:10.1016/j.cej.2018.05.186
- Gopal, N. O., Lo, H.-H., Ke, T.-F., Lee, C.-H., Chou, C.-C., Wu, J.-D., et al. (2012). Visible Light Active Phosphorus-Doped TiO<sub>2</sub> Nanoparticles: An EPR Evidence for the Enhanced Charge Separation. *J. Phys. Chem. C* 116 (30), 16191–16197. doi:10.1021/jp212346f
- Gothwal, R., and Shashidhar, T. (2015). Antibiotic Pollution in the Environment: A Review. *Clean. Soil Air Water* 43 (4), 479–489. doi:10.1002/clen.201300989
- Gudda, F. O., Waigi, M. G., Odinga, E. S., Yang, B., Carter, L., and Gao, Y. (2020). Antibiotic-contaminated Wastewater Irrigated Vegetables Pose Resistance Selection Risks to the Gut Microbiome. *Environ. Pollut.* 264, 114752. doi:10.1016/j.envpol.2020.114752
- Guinea, E., Brillas, E., Centellas, F., Cañizares, P., Rodrigo, M. A., and Sáez, C. (2009). Oxidation of Enrofloxacin with Conductive-diamond Electrochemical Oxidation, Ozonation and Fenton Oxidation. A Comparison. *Water Res.* 43 (8), 2131–2138. doi:10.1016/j.watres.2009.02.025
- Guo, F., Sun, H., Huang, X., Shi, W., and Yan, C. (2020). Fabrication of TiO<sub>2</sub>/high-Crystalline G-C<sub>3</sub>n<sub>4</sub> Composite with Enhanced Visible-Light Photocatalytic Performance for Tetracycline Degradation. *J. Chem. Techn. Biotechnol.* 95 (10), 2684–2693. doi:10.1002/jctb.6384
- He, X., Nguyen, V., Jiang, Z., Wang, D., Zhu, Z., and Wang, W.-N. (2018). Highly-oriented One-Dimensional MOF-Semiconductor Nanoarrays for Efficient Photodegradation of Antibiotics. *Catal. Sci. Technol.* 8 (8), 2117–2123. doi:10.1039/c8cy00229k
- Hirose, J., Kondo, F., Nakano, T., Kobayashi, T., Hiro, N., Ando, Y., et al. (2005). Inactivation of Antineoplastics in Clinical Wastewater by Electrolisis. *Chemosphere* 60 (8), 1018–1024. doi:10.1016/j.chemosphere.2005.01.024
- Homem, V., and Santos, L. (2011). Degradation and Removal Methods of Antibiotics from Aqueous Matrices - A Review. *J. Environ. Manage.* 92 (10), 2304–2347. doi:10.1016/j.jenvman.2011.05.023
- Hu, X., Liu, X., Tian, J., Li, Y., and Cui, H. (2017). Towards Full-Spectrum (UV, Visible, and Near-Infrared) Photocatalysis: Achieving an All-Solid-State Z-Scheme between Ag<sub>2</sub>O and TiO<sub>2</sub> Using Reduced Graphene Oxide as the Electron Mediator. *Catal. Sci. Technol.* 7 (18), 4193–4205. doi:10.1039/c7cy01349c
- Hu, X., Zhang, G., Yin, C., Li, C., and Zheng, S. (2019). Facile Fabrication of Heterogeneous TiO<sub>2</sub>/BiOCl Composite with superior Visible-Light-Driven Performance towards Cr(VI) and Tetracycline. *Mater. Res. Bull.* 119, 110559. doi:10.1016/j.materresbull.2019.110559
- Hu, X., Zhou, Q., and Luo, Y. (2010). Occurrence and Source Analysis of Typical Veterinary Antibiotics in Manure, Soil, Vegetables and Groundwater from Organic Vegetable Bases, Northern China. *Environ. Pollut.* 158 (9), 2992–2998. doi:10.1016/j.envpol.2010.05.023
- Huber, M. M., Canonica, S., Park, G.-Y., and von Gunten, U. (2003). Oxidation of Pharmaceuticals during Ozonation and Advanced Oxidation Processes. *Environ. Sci. Technol.* 37 (5), 1016–1024. doi:10.1021/es025896h
- Huo, P., Zhou, M., Tang, Y., Liu, X., Ma, C., Yu, L., et al. (2016). Incorporation of N-ZnO/CdS/Graphene Oxide Composite Photocatalyst for Enhanced Photocatalytic Activity under Visible Light. *J. Alloys Compd.* 670, 198–209. doi:10.1016/j.jallcom.2016.01.247
- Hussain, S., Naeem, M., Chaudhry, M. N., and Iqbal, M. A. (2016). Accumulation of Residual Antibiotics in the Vegetables Irrigated by Pharmaceutical Wastewater. *Expo. Health* 8 (1), 107–115. doi:10.1007/s12403-015-0186-2
- Ibhadon, A., and Fitzpatrick, P. (2013). Heterogeneous Photocatalysis: Recent Advances and Applications. *Catalysts* 3 (1), 189–218. doi:10.3390/catal3010189
- Imad Keniar, I. B., Yanni, S., Kharroubi, S., and Abou Jawdah, Y. (2021). Uptake of Gentamicin and Oxytetracycline by Plants Irrigated with Contaminated Irrigation Water. *Poster Presentation, UFWH Summit 2021* Available at <https://worldfoodcenter.ucdavis.edu/summit2021/posters-presented-viewing>.
- Jamali Alyani, S., Ebrahimian Pirbazari, A., Esmaili Khalilsaraei, F., Asasian Kolar, N., and Gilani, N. (2019). Growing Co-doped TiO<sub>2</sub> Nanosheets on Reduced Graphene Oxide for Efficient Photocatalytic Removal of Tetracycline Antibiotic from Aqueous Solution and Modeling the Process by Artificial Neural Network. *J. Alloys Compd.* 799, 169–182. doi:10.1016/j.jallcom.2019.05.175
- Jammoul, A., and El Darra, N. (2019). Evaluation of Antibiotics Residues in Chicken Meat Samples in Lebanon. *Antibiotics (Basel)* 8 (2), 69. doi:10.3390/antibiotics8020069
- Jiao, S., Zheng, S., Yin, D., Wang, L., and Chen, L. (2008). Aqueous Oxytetracycline Degradation and the Toxicity Change of Degradation Compounds in Photoirradiation Process. *J. Environ. Sci.* 20 (7), 806–813. doi:10.1016/s1001-0742(08)62130-0
- Jin, Y., Jiang, D., Li, D., and Chen, M. (2017). Construction of Ultrafine TiO<sub>2</sub> Nanoparticle and SnNb<sub>2</sub>O<sub>6</sub> Nanosheet 0D/2D Heterojunctions with Abundant Interfaces and Significantly Improved Photocatalytic Activity. *Catal. Sci. Technol.* 7 (11), 2308–2317. doi:10.1039/c7cy00366h
- Jo, W.-K., Kumar, S., Isaacs, M. A., Lee, A. F., and Karthikeyan, S. (2017). Cobalt Promoted TiO<sub>2</sub>/GO for the Photocatalytic Degradation of Oxytetracycline and Congo Red. *Appl. Catal. B: Environ.* 201, 159–168. doi:10.1016/j.apcatb.2016.08.022
- Khodadoost, S., Hadi, A., Karimi-Sabet, J., Mehdipourghazi, M., and Golzary, A. (2017). Optimization of Hydrothermal Synthesis of Bismuth Titanate Nanoparticles and Application for Photocatalytic Degradation of Tetracycline. *J. Environ. Chem. Eng.* 5 (6), 5369–5380. doi:10.1016/j.jece.2017.10.006
- Kim, S. H., Shon, H. K., and Ngo, H. H. (2010). Adsorption Characteristics of Antibiotics Trimethoprim on Powdered and Granular Activated Carbon. *J. Ind. Eng. Chem.* 16 (3), 344–349. doi:10.1016/j.jiec.2009.09.061
- Klauson, D., Babkina, J., Stepanova, K., Krichevskaya, M., and Preis, S. (2010). Aqueous Photocatalytic Oxidation of Amoxicillin. *Catal. Today* 151 (1), 39–45. doi:10.1016/j.cattod.2010.01.015
- Koe, W. S., Lee, J. W., Chong, W. C., Pang, Y. L., and Sim, L. C. (2019). An Overview of Photocatalytic Degradation: Photocatalysts, Mechanisms, and Development of Photocatalytic Membrane. *Environ. Sci. Pollut. Res. Int.* 27, 2522–2565. doi:10.1007/s11356-019-07193-5
- Kosutic, K., Dolar, D., Asperger, D., and Kunst, B. (2007). Removal of Antibiotics from a Model Wastewater by RO/NF Membranes. *Separat. Purif. Techn.* 53 (3), 244–249. doi:10.1016/j.seppur.2006.07.015
- Koyuncu, I., Arikon, O. A., Wiesner, M. R., and Riceb, C. (2008). Removal of Hormones and Antibiotics by Nanofiltration Membranes. *J. Membr. Sci.* 309 (1), 94–101. doi:10.1016/j.memsci.2007.10.010

- Lakhera, S. K., Hafeez, H. Y., Veluswamy, P., Ganesh, V., Khan, A., Ikeda, H., et al. (2018). Enhanced Photocatalytic Degradation and Hydrogen Production Activity of *In Situ* Grown TiO<sub>2</sub> Coupled NiTiO<sub>3</sub> Nanocomposites. *Appl. Surf. Sci.* 449, 790–798. doi:10.1016/j.apsusc.2018.02.136
- Li, C., Hu, R., Lu, X., Bashir, S., and Liu, J. L. (2020). Efficiency Enhancement of Photocatalytic Degradation of Tetracycline Using Reduced Graphene Oxide Coordinated Titania Nanoplatelet. *Catal. Today* 350, 171–183. doi:10.1016/j.cattod.2019.06.038
- Li, D., and Shi, W. (2016). Recent Developments in Visible-Light Photocatalytic Degradation of Antibiotics. *Chin. J. Catal.* 37 (6), 792–799. doi:10.1016/s1872-2067(15)61054-3
- Li, J., Liu, K., Xue, J., Xue, G., Sheng, X., Wang, H., et al. (2019). CQDS Pseudocapacitor-Incorporated 3D Burger-like Hybrid ZnO Enhanced Visible-Light-Driven Photocatalytic Activity and Mechanism Implication. *J. Catal.* 369, 450–461. doi:10.1016/j.jcat.2018.11.026
- Li, J., Zhou, M., Ye, Z., Wang, H., Ma, C., Huo, P., et al. (2015). Enhanced Photocatalytic Activity of G-C<sub>3</sub>N<sub>4</sub>-ZnO/HNT Composite Heterostructure Photocatalysts for Degradation of Tetracycline under Visible Light Irradiation. *RSC Adv.* 5 (111), 91177–91189. doi:10.1039/c5ra17360d
- Li, K., Yediler, A., Yang, M., Schulte-Hostede, S., and Wong, M. H. (2008). Ozonation of Oxytetracycline and Toxicological Assessment of its Oxidation By-Products. *Chemosphere* 72 (3), 473–478. doi:10.1016/j.chemosphere.2008.02.008
- Li, L., Jinling, S., Baoying, W., Chenglin, D., Ruifen, W., and Bangwen, Z. (2019). A New BiOXs/TiO<sub>2</sub> Heterojunction Photocatalyst towards Efficient Degradation of Organic Pollutants under Visible-Light Irradiation. *Micro Nano Lett.* 14, 911–914. doi:10.1049/mnl.2018.5584
- Li, R., Li, T., and Zhou, Q. (2020). Impact of Titanium Dioxide (TiO<sub>2</sub>) Modification on its Application to Pollution Treatment-A Review. *Catalysts* 10 (7), 804. doi:10.3390/catal10070804
- Li, W., Ding, H., Ji, H., Dai, W., Guo, J., and Du, G. (2018). Photocatalytic Degradation of Tetracycline Hydrochloride via a CdS-TiO<sub>2</sub> Heterostructure Composite under Visible Light Irradiation. *Nanomaterials* 8 (6), 415. doi:10.3390/nano8060415
- Li, W., Li, B., Meng, M., Cui, Y., Wu, Y., Zhang, Y., et al. (2019). Bimetallic Au/Ag Decorated TiO<sub>2</sub> Nanocomposite Membrane for Enhanced Photocatalytic Degradation of Tetracycline and Bactericidal Efficiency. *Appl. Surf. Sci.* 487, 1008–1017. doi:10.1016/j.apsusc.2019.05.162
- Liao, X., Li, T.-T., Ren, H.-T., Mao, Z., Zhang, X., Lin, J.-H., et al. (2021). Enhanced Photocatalytic Performance through the Ferroelectric Synergistic Effect of P-N Heterojunction BiFeO<sub>3</sub>/TiO<sub>2</sub> under Visible-Light Irradiation. *Ceramics Int.* 47 (8), 10786–10795. doi:10.1016/j.ceramint.2020.12.195
- Libralato, G., Lofrano, G., Siciliano, A., Gambino, E., Boccia, G., Federica, C., et al. (2020). “Toxicity Assessment of Wastewater after Advanced Oxidation Processes for Emerging Contaminants’ Degradation,” in *Visible Light Active Structured Photocatalysts for the Removal of Emerging Contaminants*. Editors O. Sacco and V. Vaiano (Elsevier), 195–211. doi:10.1016/b978-0-12-818334-2.00008-0
- Liu, C., Dong, S., and Chen, Y. (2019). Enhancement of Visible-Light-Driven Photocatalytic Activity of Carbon Plane/g-C<sub>3</sub>N<sub>4</sub>/TiO<sub>2</sub> Nanocomposite by Improving Heterojunction Contact. *Chem. Eng. J.* 371, 706–718. doi:10.1016/j.cej.2019.04.089
- Liu, C., Wu, G., Chen, J., Huang, K., and Shi, W. (2016). Fabrication of a Visible-Light-Driven Photocatalyst and Degradation of Tetracycline Based on the Photoinduced Interfacial Charge Transfer of SrTiO<sub>3</sub>/Fe<sub>2</sub>O<sub>3</sub> Nanowires. *New J. Chem.* 40 (6), 5198–5208. doi:10.1039/c5nj03167b
- Liu, M., Shuili, Y., Hou, L., and Xiaojun, H. (2019). Removal of Oxytetracycline by Fe<sub>2</sub>O<sub>3</sub>-TiO<sub>2</sub>/modified Zeolite Composites under Visible Light Irradiation. *J. Mater. Sci. Mater. Electro.* 30, 9087–9096. doi:10.1007/s10854-019-01052-2
- Liu, W., Dai, Z., Liu, Y., Zhu, A., Zhong, D., Wang, J., et al. (2018). Intimate Contacted Two-Dimensional/zero-Dimensional Composite of Bismuth Titanate Nanosheets Supported Ultrafine Bismuth Oxychloride Nanoparticles for Enhanced Antibiotic Residue Degradation. *J. Colloid Interf. Sci.* 529, 23–33. doi:10.1016/j.jcis.2018.05.112
- Liu, X., Lv, P., Yao, G., Ma, C., Huo, P., and Yan, Y. (2013). Microwave-assisted Synthesis of Selective Degradation Photocatalyst by Surface Molecular Imprinting Method for the Degradation of Tetracycline onto CITiO<sub>2</sub>. *Chem. Eng. J.* 217, 398–406. doi:10.1016/j.cej.2012.12.007
- Liu, Y., Tian, J., Wang, Q., Wei, L., Wang, C., and Yang, C. (2020). Enhanced Visible Light Photocatalytic Activity of G-C<sub>3</sub>N<sub>4</sub> via the Synergistic Effect of K Atom Bridging Doping and Nanosheets Formed by thermal Exfoliation. *Opt. Mater.* 99, 109594. doi:10.1016/j.optmat.2019.109594
- Liu, Y., Tian, J., Wei, L., Wang, Q., Wang, C., Xing, Z., et al. (2021). Modified G-C<sub>3</sub>N<sub>4</sub>/TiO<sub>2</sub>/CdS Ternary Heterojunction Nanocomposite as Highly Visible Light Active Photocatalyst Originated from CdS as the Electron Source of TiO<sub>2</sub> to Accelerate Z-type Heterojunction. *Separat. Purif. Techn.* 257, 117976. doi:10.1016/j.seppur.2020.117976
- Low, J., Yu, J., Jaromic, M., Wageh, S., and Al-Ghamdi, A. A. (2017). Heterojunction Photocatalysts. *Adv. Mater.* 29 (20), 1601694. doi:10.1002/adma.201601694
- Lyu, J., Zhou, Z., Wang, Y., Li, J., Li, Q., Zhang, Y., et al. (2019). Platinum-enhanced Amorphous TiO<sub>2</sub>-Filled Mesoporous TiO<sub>2</sub> Crystals for the Photocatalytic Mineralization of Tetracycline Hydrochloride. *J. Hazard. Mater.* 373, 278–284. doi:10.1016/j.jhazmat.2019.03.096
- Ma, S., Gu, J., Han, Y., Gao, Y., Zong, Y., Ye, Z., et al. (2019). Facile Fabrication of C-TiO<sub>2</sub> Nanocomposites with Enhanced Photocatalytic Activity for Degradation of Tetracycline. *ACS Omega* 4 (25), 21063–21071. doi:10.1021/acsomega.9b02411
- Mahdavi, H., Sajedi, M., Shahalizade, T., Heidari, A. A., and Bulletin, P. (2019). Preparation and Application of Catalytic Polymeric Membranes Based on PVDF/cobalt Nanoparticles Supported on MWCNTs. *Polym. Bull.* 77, 4489–4505. doi:10.1007/s00289-019-02983-w
- Marcelino, R. B. P., and Amorim, C. C. (2019). Towards Visible-Light Photocatalysis for Environmental Applications: Band-gap Engineering versus Photons Absorption-A Review. *Environ. Sci. Pollut. Res.* 26 (5), 4155–4170. doi:10.1007/s11356-018-3117-5
- Marchelek, M., Diak, M., Kozak, M., Zaleska-Medynska, A., and Grabowska, E. (2016). “Some Unitary, Binary, and Ternary Non-TiO<sub>2</sub> Photocatalysts,” in *Semiconductor Photocatalysis - Materials, Mechanisms and Applications*.
- Marschall, R., and Wang, L. (2014). Non-metal Doping of Transition Metal Oxides for Visible-Light Photocatalysis. *Catal. Today* 225, 111–135. doi:10.1016/j.cattod.2013.10.088
- Minala, M., Gu, Z., Guadie, A., Kabtamu, D. M., Li, Y., and Wang, X. (2020). Application of Graphene-Based Materials for Removal of Tetracyclines Using Adsorption and Photocatalytic-Degradation: A Review. *J. Environ. Manage.* 276, 111310. doi:10.1016/j.jenvman.2020.111310
- Mohd Adnan, M. A., Muhd Julkapli, N., Amir, M. N. I., and Maamor, A. (2018). Effect on Different TiO<sub>2</sub> Photocatalyst Supports on Photodecolorization of Synthetic Dyes: a Review. *Int. J. Environ. Sci. Technol.* 16, 547–566. doi:10.1007/s13762-018-1857-x
- Mokh, S., El Hawari, K., Rahim, H. A., Al Iskandarani, M., and Jaber, F. (2020). Antimicrobial Residues Survey by LC-MS in Food-Producing Animals in Lebanon. *Food Additives & Contaminants: B* 13 (2), 121–129. doi:10.1080/19393210.2020.1739148
- Mokh, S., El Khatib, M., Koubar, M., Daher, Z., and Al Iskandarani, M. (2017). Innovative SPE-LC-MS/MS Technique for the Assessment of 63 Pharmaceuticals and the Detection of Antibiotic-Resistant-Bacteria: A Case Study Natural Water Sources in Lebanon. *Sci. Total Environ.* 609, 830–841. doi:10.1016/j.scitotenv.2017.07.230
- Mokhtari Nesfchi, M., Ebrahimian Pirbazari, A., Khalil Saraei, F. E., Rojaee, F., Mahdavi, F., and Fa’al Rastegar, S. A. (2021). Fabrication of Plasmonic Nanoparticles/Cobalt Doped TiO<sub>2</sub> Nanosheets for Degradation of Tetracycline and Modeling the Process by Artificial Intelligence Techniques. *Mater. Sci. Semiconductor Process.* 122, 105465. doi:10.1016/j.mssp.2020.105465
- Mousavi, M., and Ghasemi, J. B. (2021). Novel Visible-Light-Responsive Black-TiO<sub>2</sub>/CoTiO<sub>3</sub> Z-Scheme Heterojunction Photocatalyst with Efficient Photocatalytic Performance for the Degradation of Different Organic Dyes and Tetracycline. *J. Taiwan Inst. Chem. Eng.* 121, 168–183. doi:10.1016/j.jtice.2021.04.009

- Navalon, S., Alvaro, M., and Garcia, H. (2008). Reaction of Chlorine Dioxide with Emergent Water Pollutants: Product Study of the Reaction of Three Beta-Lactam Antibiotics with ClO<sub>2</sub>. *Water Res.* 42 (8), 1935–1942. doi:10.1016/j.watres.2007.11.023
- Niu, J., Ding, S., Zhang, L., Zhao, J., and Feng, C. (2013). Visible-light-mediated Sr-Bi<sub>2</sub>O<sub>3</sub> Photocatalysis of Tetracycline: Kinetics, Mechanisms and Toxicity Assessment. *Chemosphere* 93 (1), 1–8. doi:10.1016/j.chemosphere.2013.04.043
- Niu, J., Lu, P., Kang, M., Deng, K., Yao, B., Yu, X., et al. (2014). P-doped TiO<sub>2</sub> with superior Visible-Light Activity Prepared by Rapid Microwave Hydrothermal Method. *Appl. Surf. Sci.* 319, 99–106. doi:10.1016/j.apsusc.2014.07.048
- Niu, X., Yan, W., Shao, C., Zhao, H., and Yang, J. (2019). Hydrothermal Synthesis of Mo-C Co-doped TiO<sub>2</sub> and Coupled with Fluorine-Doped Tin Oxide (FTO) for High-Efficiency Photodegradation of Methylene Blue and Tetracycline: Effect of Donor-Acceptor Passivated Co-doping. *Appl. Surf. Sci.* 466, 882–892. doi:10.1016/j.apsusc.2018.10.019
- Oseghe, E. O., and Ofomaja, A. E. (2018a). Facile Microwave Synthesis of pine Cone Derived C-Doped TiO<sub>2</sub> for the Photodegradation of Tetracycline Hydrochloride under Visible-LED Light. *J. Environ. Manage.* 223, 860–867. doi:10.1016/j.jenvman.2018.07.003
- Oseghe, E. O., and Ofomaja, A. E. (2018b). Study on Light Emission Diode/carbon Modified TiO<sub>2</sub> System for Tetracycline Hydrochloride Degradation. *J. Photochem. Photobiol. A: Chem.* 360, 242–248. doi:10.1016/j.jphotochem.2018.04.048
- Ouyang, W., and Ji, Y. (2020). Facile Route for Porous N,S Co-doped TiO<sub>2</sub> Nanoparticles for Visible Light-driven Photocatalysis. *Micro Nano Lett.* 15 (8), 566–569. doi:10.1049/mnl.2020.0152
- Palanivelu, K., Im, J.-S., and Lee, Y.-S. (2007). Carbon Doping of TiO<sub>2</sub> for Visible Light Photo Catalysis - A Review. *Carbon Lett.* 8, 214–224. doi:10.5714/cl.2007.8.3.214
- Pan, M., and Chu, L. M. (2017). Fate of Antibiotics in Soil and Their Uptake by Edible Crops. *Sci. Total Environ.* 599–600, 500–512. doi:10.1016/j.scitotenv.2017.04.214
- Pan, M., Wong, C. K. C., and Chu, L. M. (2014). Distribution of Antibiotics in Wastewater-Irrigated Soils and Their Accumulation in Vegetable Crops in the Pearl River Delta, Southern China. *J. Agric. Food Chem.* 62 (46), 11062–11069. doi:10.1021/jf503850v
- Pang, S., Huang, J.-g., Su, Y., Geng, B., Lei, S.-y., Huang, Y.-t., et al. (2016). Synthesis and Modification of Zn-Doped TiO<sub>2</sub> Nanoparticles for the Photocatalytic Degradation of Tetracycline. *Photochem. Photobiol.* 92 (5), 651–657. doi:10.1111/php.12626
- Pouretedal, H. R., and Afshari, B. (2016). Preparation and Characterization of Zr and Sn Doped TiO<sub>2</sub> Nanocomposite and Photocatalytic Activity in Degradation of Tetracycline. *Desalination Water Treat.* 57 (23), 10941–10947. doi:10.1080/19443994.2015.1041056
- Pudukudy, M., Jia, Q., Yuan, J., Megala, S., Rajendran, R., and Shan, S. (2020). Influence of CeO<sub>2</sub> Loading on the Structural, Textural, Optical and Photocatalytic Properties of Single-Pot Sol-Gel Derived Ultrafine CeO<sub>2</sub>/TiO<sub>2</sub> Nanocomposites for the Efficient Degradation of Tetracycline under Visible Light Irradiation. *Mater. Sci. Semiconductor Process.* 108, 104891. doi:10.1016/j.mssp.2019.104891
- Radjenović, J., Petrović, M., Ventura, F., and Barceló, D. (2008). Rejection of Pharmaceuticals in Nanofiltration and Reverse Osmosis Membrane Drinking Water Treatment. *Water Res.* 42 (14), 3601–3610. doi:10.1016/j.watres.2008.05.020
- Radwan, E. K., Langford, C. H., and Achari, G. (2018). Impact of Support Characteristics and Preparation Method on Photocatalytic Activity of TiO<sub>2</sub>/ZSM-5/silica Gel Composite Photocatalyst. *R. Soc. Open Sci.* 5 (9), 180918. doi:10.1098/rsos.180918
- Raschid-Sally, L., and Jayakody, P. (2008). *Drivers and Characteristics of Wastewater Agriculture in Developing Countries: Results from a Global Assessment*. Colombi, Sri Lanka: International Water Management Institute.
- Rasheed, H. U., Lv, X., Wei, W., Yaseen, W., Ullah, N., Xie, J., et al. (2019). Synthesis and Studies of ZnO Doped with G-C<sub>3</sub>N<sub>4</sub> Nanocomposites for the Degradation of Tetracycline Hydrochloride under the Visible Light Irradiation. *J. Environ. Chem. Eng.* 7 (3), 103152. doi:10.1016/j.jece.2019.103152
- Rimoldi, L., Pargoletti, E., Meroni, D., Falletta, E., Cerrato, G., Turco, F., et al. (2018). Concurrent Role of Metal (Sn, Zn) and N Species in Enhancing the Photocatalytic Activity of TiO<sub>2</sub> under Solar Light. *Catal. Today* 313, 40–46. doi:10.1016/j.cattod.2017.12.017
- Robles Jimenez, L. E., Angeles Hernandez, J. C., Osorio Avalos, J., Li, X., Atwill, E. R., Castelan Ortega, O., et al. (2019). “Veterinary Antibiotics in Animal Diet: Effects on Waste/Environment,” in *Bioactive Molecules in Food*. Editors J.-M. Mérillon and K. G. Ramawat (Cham: Springer International Publishing), 1775–1792. doi:10.1007/978-3-319-78030-6\_41
- Saadati, F., Keramati, N., and Ghazi, M. M. (2016a). Influence of Parameters on the Photocatalytic Degradation of Tetracycline in Wastewater: A Review. *Crit. Rev. Environ. Sci. Techn.* 46 (8), 757–782. doi:10.1080/10643389.2016.1159093
- Saadati, F., Keramati, N., and Mehdipour ghazi, M. (2016b). Synthesis of Nanocomposite Based on Semnan Natural Zeolite for Photocatalytic Degradation of Tetracycline under Visible Light. *Adv. Environ. Techn.* 2 (2), 63–70. doi:10.22104/aet.2016.399
- Safari, G. H., Hoseini, M., Seyedsalehi, M., Kamani, H., Jaafari, J., and Mahvi, A. H. (2014). Photocatalytic Degradation of Tetracycline Using Nanosized Titanium Dioxide in Aqueous Solution. *Int. J. Environ. Sci. Technol.* 12 (2), 603–616. doi:10.1007/s13762-014-0706-9
- Sanganyado, E., and Gwenzi, W. (2019). Antibiotic Resistance in Drinking Water Systems: Occurrence, Removal, and Human Health Risks. *Sci. Total Environ.* 669, 785–797. doi:10.1016/j.scitotenv.2019.03.162
- Scaria, J., Karim, A. V., Divyapriya, G., Nidheesh, P. V., and Suresh Kumar, M. (2020). “Carbon-supported Semiconductor Nanoparticles as Effective Photocatalysts for Water and Wastewater Treatment,” in *Nano-Materials as Photocatalysts for Degradation of Environmental Pollutants*. Editor P. Singh (Elsevier), 245–278. doi:10.1016/b978-0-12-818598-8.00013-4
- Shen, J., Xue, J., Chen, Z., Ni, J., Tang, B., He, G., et al. (2018). One-step Hydrothermal Synthesis of Peony-like Ag/Bi<sub>2</sub>WO<sub>6</sub> as Efficient Visible Light-Driven Photocatalyst toward Organic Pollutants Degradation. *J. Mater. Sci.* 53 (7), 4848–4860. doi:10.1007/s10853-017-1885-9
- Singh, R., Singh, A. P., Kumar, S., Giri, B. S., and Kim, K.-H. (2019). Antibiotic Resistance in Major Rivers in the World: A Systematic Review on Occurrence, Emergence, and Management Strategies. *J. Clean. Prod.* 234, 1484–1505. doi:10.1016/j.jclepro.2019.06.243
- Sommer, M. E., Elgeti, M., Hildebrand, P. W., Szczepek, M., Hofmann, K. P., and Scheerer, P. (2015). “Structure-Based Biophysical Analysis of the Interaction of Rhodopsin with G Protein and Arrestin,” in *Methods in Enzymology*. Editor A. K. Shukla (Academic Press), 563–608. doi:10.1016/bs.mie.2014.12.014
- Song, J., Wu, X., Zhang, M., Liu, C., Yu, J., Sun, G., et al. (2020). Highly Flexible, Core-Shell Heterostructured, and Visible-Light-Driven Titania-Based Nanofibrous Membranes for Antibiotic Removal and E. Coli Inactivation. *Chem. Eng. J.* 379, 122269. doi:10.1016/j.cej.2019.122269
- Sponza, D. T., and Koyuncuoglu, P. (2019). Photodegradation of Ciprofloxacin and Ofloxacin Antibiotics and Their Photo-Metabolites with Sunlight. *Clin. Microbiol. Infect. Dis.* 4. doi:10.15761/cm.1000149
- Stackelberg, P. E., Gibs, J., Furlong, E. T., Meyer, M. T., Zaugg, S. D., and Lippincott, R. L. (2007). Efficiency of Conventional Drinking-Water-Treatment Processes in Removal of Pharmaceuticals and Other Organic Compounds. *Sci. Total Environ.* 377 (2), 255–272. doi:10.1016/j.scitotenv.2007.01.095
- Sun, J., Huang, D., Liu, R., Dai, J., and Chen, J. (2019). Photocatalytic Performance of Ag/AgBr Modified TiO<sub>2</sub>: Critical Impacts and Wastewater Sample Study. *J. Mater. Sci. Mater. Electron.* 30 (16), 15754–15765. doi:10.1007/s10854-019-01961-2
- Sundar, K. P., and Kanmani, S. (2020). Progression of Photocatalytic Reactors and It's Comparison: A Review. *Chem. Eng. Res. Des.* 154, 135–150. doi:10.1016/j.cherd.2019.11.035
- Tabatabai-Yazdi, F. S., Ebrahimi Pirbazari, A., Esmaeili Khalilsaraei, F., Asasian Kolur, N., and Gilani, N. (2020). Photocatalytic Treatment of Tetracycline Antibiotic Wastewater by silver/TiO<sub>2</sub> Nanosheets/reduced Graphene Oxide and Artificial Neural Network Modeling. *Water Environ. Res.* 92 (5), 662–676. doi:10.1002/wer.1258
- Tang, X., Wang, Z., and Wang, Y. (2018). Visible Active N-Doped TiO<sub>2</sub>/reduced Graphene Oxide for the Degradation of Tetracycline Hydrochloride. *Chem. Phys. Lett.* 691, 408–414. doi:10.1016/j.cplett.2017.11.037
- Teoh, W. Y., Scott, J. A., and Amal, R. (2012). Progress in Heterogeneous Photocatalysis: From Classical Radical Chemistry to Engineering Nanomaterials and Solar Reactors. *J. Phys. Chem. Lett.* 3 (5), 629–639. doi:10.1021/jz3000646

- Tong, H., Ouyang, S., Bi, Y., Umezawa, N., Oshikiri, M., and Ye, J. (2012). Nano-photocatalytic Materials: Possibilities and Challenges. *Adv. Mater.* 24 (2), 229–251. doi:10.1002/adma.201102752
- Vázquez, A., Hernández-Uresti, D. B., and Obregón, S. (2016). Electrophoretic Deposition of CdS Coatings and Their Photocatalytic Activities in the Degradation of Tetracycline Antibiotic. *Appl. Surf. Sci.* 386, 412–417. doi:10.1016/j.apsusc.2016.06.034
- Vieno, N. M., Härkki, H., Tuhkanen, T., and Kronberg, L. (2007). Occurrence of Pharmaceuticals in River Water and Their Elimination in a Pilot-Scale Drinking Water Treatment Plant. *Environ. Sci. Technol.* 41 (14), 5077–5084. doi:10.1021/es062720x
- Wang, C., Wu, Y., Lu, J., Zhao, J., Cui, J., Wu, X., et al. (2017). Bioinspired Synthesis of Photocatalytic Nanocomposite Membranes Based on Synergy of Au-TiO<sub>2</sub> and Polydopamine for Degradation of Tetracycline under Visible Light. *ACS Appl. Mater. Inter.* 9 (28), 23687–23697. doi:10.1021/acsami.7b04902
- Wang, H., Wu, D., Li, X., and Huo, P. (2019). Ce Doping TiO<sub>2</sub>/halloysite Nanotubes Photocatalyst for Enhanced Electrons Transfer and Photocatalytic Degradation of Tetracycline. *J. Mater. Sci. Mater. Electron.* 30 (21), 19126–19136. doi:10.1007/s10854-019-02268-y
- Wang, P., Yap, P.-S., and Lim, T.-T. (2011). C–N–S Tridoped TiO<sub>2</sub> for Photocatalytic Degradation of Tetracycline under Visible-Light Irradiation. *Appl. Catal. A: Gen.* 399 (1), 252–261. doi:10.1016/j.apcata.2011.04.008
- Wang, T., Quan, W., Jiang, D., Chen, L., Li, D., Meng, S., et al. (2016). Synthesis of Redox-mediator-free Direct Z-Scheme AgI/WO<sub>3</sub> Nanocomposite Photocatalysts for the Degradation of Tetracycline with Enhanced Photocatalytic Activity. *Chem. Eng. J.* 300, 280–290. doi:10.1016/j.cej.2016.04.128
- Wang, T., Zhong, S., Zou, S., Jiang, F., Feng, L., and Su, X. (2017). Novel Bi<sub>2</sub>WO<sub>6</sub>-coupled Fe<sub>3</sub>O<sub>4</sub> Magnetic Photocatalysts: Preparation, Characterization and Photodegradation of Tetracycline Hydrochloride. *Photochem. Photobiol.* 93 (4), 1034–1042. doi:10.1111/php.12739
- Wang, W., Xiao, K., Zhu, L., Yin, Y., and Wang, Z. (2017). Graphene Oxide Supported Titanium Dioxide & Ferroferric Oxide Hybrid, a Magnetically Separable Photocatalyst with Enhanced Photocatalytic Activity for Tetracycline Hydrochloride Degradation. *RSC Adv.* 7 (34), 21287–21297. doi:10.1039/c6ra28224e
- Wei, Z., Liu, J., and Shangguan, W. (2020). A Review on Photocatalysis in Antibiotic Wastewater: Pollutant Degradation and Hydrogen Production. *Chin. J. Catal.* 41 (10), 1440–1450. doi:10.1016/s1872-2067(19)63448-0
- Wu, G., Li, P., Xu, D., Luo, B., Hong, Y., Shi, W., et al. (2015). Hydrothermal Synthesis and Visible-Light-Driven Photocatalytic Degradation for Tetracycline of Mn-Doped SrTiO<sub>3</sub> Nanocubes. *Appl. Surf. Sci.* 333, 39–47. doi:10.1016/j.apsusc.2015.02.008
- Wu, Q. (2019). The Fabrication of Magnetic Recyclable Nitrogen Modified Titanium Dioxide/strontium Ferrite/diatomite Heterojunction Nanocomposite for Enhanced Visible-Light-Driven Photodegradation of Tetracycline. *Int. J. Hydrogen Energ.* 44 (16), 8261–8272. doi:10.1016/j.ijhydene.2019.01.145
- Wu, S., Hu, H., Lin, Y., Zhang, J., and Hu, Y. H. (2020). Visible Light Photocatalytic Degradation of Tetracycline over TiO<sub>2</sub>. *Chem. Eng. J.* 382, 122842. doi:10.1016/j.cej.2019.122842
- Wu, X., Yin, S., Dong, Q., Guo, C., Li, H., Kimura, T., et al. (2013). Synthesis of High Visible Light Active Carbon Doped TiO<sub>2</sub> Photocatalyst by a Facile Calcination Assisted Solvothermal Method. *Appl. Catal. B: Environ.* 142–143, 450–457. doi:10.1016/j.apcatb.2013.05.052
- Xu, H., Ding, Y., Yang, S., Zhang, H., Wang, X., Yuan, J., et al. (2021). Carbon-doped Titania-Polymethylsilsesquioxane Aerogels for the Photocatalytic Degradation of Antibiotics. *Bull. Mater. Sci.* 44 (3), 226. doi:10.1007/s12034-021-02510-6
- Xu, L., Zhang, H., Xiong, P., Zhu, Q., Liao, C., and Jiang, G. (2021). Occurrence, Fate, and Risk Assessment of Typical Tetracycline Antibiotics in the Aquatic Environment: A Review. *Sci. Total Environ.* 753, 141975. doi:10.1016/j.scitotenv.2020.141975
- Xu, P., Shen, X., Luo, L., Shi, Z., Liu, Z., Chen, Z., et al. (2018). Preparation of TiO<sub>2</sub>/Bi<sub>2</sub>WO<sub>6</sub> Nanostructured Heterojunctions on Carbon Fibers as a Weaveable Visible-Light Photocatalyst/Photoelectrode. *Environ. Sci. Nano* 5 (2), 327–337. doi:10.1039/c7en00822h
- Yan, Q., Li, C., Lin, C., Zhao, Y., and Zhang, M. (2018). Visible Light Response AgBr/Ag<sub>3</sub>PO<sub>4</sub> Hybrid for Removal of Anionic Dye and Tetracycline Hydrochloride in Water. *J. Mater. Sci. Mater. Electron.* 29 (3), 2517–2524. doi:10.1007/s10854-017-8174-x
- Yan, S., Yang, J., Li, Y., Jia, X., and Song, H. (2020). One-step Synthesis of ZnS/BiOBr Photocatalyst to Enhance Photodegradation of Tetracycline under Full Spectral Irradiation. *Mater. Lett.* 276, 128232. doi:10.1016/j.matlet.2020.128232
- Yang, W., Vogler, B., Lei, Y., and Wu, T. (2017). Metallic Ion Leaching from Heterogeneous Catalysts: an Overlooked Effect in the Study of Catalytic Ozonation Processes. *Environ. Sci. Water Res. Technol.* 3 (6), 1143–1151. doi:10.1039/c7ew00273d
- Yang, X., Chen, Z., Zhao, W., Liu, C., Qian, X., Zhang, M., et al. (2021). Recent Advances in Photodegradation of Antibiotic Residues in Water. *Chem. Eng. J.* 405, 126806. doi:10.1016/j.cej.2020.126806
- You, J., Guo, Y., Guo, R., and Liu, X. (2019). A Review of Visible Light-Active Photocatalysts for Water Disinfection: Features and Prospects. *Chem. Eng. J.* 373, 624–641. doi:10.1016/j.cej.2019.05.071
- Yu, X., Lu, Z., Si, N., Zhou, W., Chen, T., Gao, X., et al. (2014). Preparation of Rare Earth Metal ion/TiO<sub>2</sub>Hal-Conducting Polymers by Ions Imprinting Technique and its Photodegradation Property on Tetracycline. *Appl. Clay Sci.* 99, 125–130. doi:10.1016/j.clay.2014.06.021
- Yuan, J., Pudukudy, M., Hu, T., Liu, Y., Luo, X., Zhi, Y., et al. (2021). CeOx-coupled MIL-125-Derived C-TiO<sub>2</sub> Catalysts for the Enhanced Photocatalytic Abatement of Tetracycline under Visible Light Irradiation. *Appl. Surf. Sci.* 557, 149829. doi:10.1016/j.apsusc.2021.149829
- Zeghiod, H., Khellaf, N., Djelal, H., Amrane, A., and Bouhlassa, M. (2016). Photocatalytic Reactors Dedicated to the Degradation of Hazardous Organic Pollutants: Kinetics, Mechanistic Aspects, and Design - A Review. *Chem. Eng. Commun.* 203 (11), 1415–1431. doi:10.1080/00986445.2016.1202243
- Zhang, B., He, X., Ma, X., Chen, Q., Liu, G., Zhou, Y., et al. (2020). *In Situ* synthesis of Ultrafine TiO<sub>2</sub> Nanoparticles Modified G-C<sub>3</sub>n<sub>4</sub> Heterojunction Photocatalyst with Enhanced Photocatalytic Activity. *Separat. Purif. Technol.* 247, 116932. doi:10.1016/j.seppur.2020.116932
- Zhang, F. J., Li, R. S., Li, J. M., Liu, C. J., Jiang, C., and Kang, C. L. (2017). Preparation of Zn Doped TiO<sub>2</sub> Nanoparticles Decorated on Graphene F or Photocatalytic Degradation of Tetracycline. *Optoelectronics Adv. Materials-Rapid Commun.* 11 (January-February 2017), 88–95.
- Zhang, F., Wang, X., Liu, H., Liu, C., Wan, Y., Long, Y., et al. (2019). Recent Advances and Applications of Semiconductor Photocatalytic Technology. *Appl. Sci.* 9 (12), 2489. doi:10.3390/app9122489
- Zhang, G., Guan, W., Shen, H., Zhang, X., Fan, W., Lu, C., et al. (2014). Organic Additives-free Hydrothermal Synthesis and Visible-Light-Driven Photodegradation of Tetracycline of WO<sub>3</sub> Nanosheets. *Ind. Eng. Chem. Res.* 53 (13), 5443–5450. doi:10.1021/ie4036687
- Zhang, G., Ji, S., and Xi, B. (2006). Feasibility Study of Treatment of Amoxicillin Wastewater with a Combination of Extraction, Fenton Oxidation and Reverse Osmosis. *Desalination* 196 (1), 32–42. doi:10.1016/j.desal.2005.11.018
- Zhang, Q.-Q., Ying, G.-G., Pan, C.-G., Liu, Y.-S., and Zhao, J.-L. (2015). Comprehensive Evaluation of Antibiotics Emission and Fate in the River Basins of China: Source Analysis, Multimedia Modeling, and Linkage to Bacterial Resistance. *Environ. Sci. Technol.* 49 (11), 6772–6782. doi:10.1021/acs.est.5b00729
- Zhang, S., Xu, J., Hu, J., Cui, C., and Liu, H. (2017). Interfacial Growth of TiO<sub>2</sub>-rGO Composite by Pickering Emulsion for Photocatalytic Degradation. *Langmuir* 33 (20), 5015–5024. doi:10.1021/acs.langmuir.7b00719
- Zhang, S., Yin, Z., Xie, L., Yi, J., Tang, W., Tang, T., et al. (2020). Facet Engineered TiO<sub>2</sub> Hollow Sphere for the Visible-Light-Mediated Degradation of Antibiotics via Ligand-To-Metal Charge Transfer. *Ceramics Int.* 46 (7), 8949–8957. doi:10.1016/j.ceramint.2019.12.142
- Zhang, T., Liu, Y., Rao, Y., Li, X., Yuan, D., Tang, S., et al. (2020). Enhanced Photocatalytic Activity of TiO<sub>2</sub> with Acetylene Black and Persulfate for Degradation of Tetracycline Hydrochloride under Visible Light. *Chem. Eng. J.* 384, 123350. doi:10.1016/j.cej.2019.123350
- Zheng, X., Fu, W., Kang, F., Peng, H., and Wen, J. (2018). Enhanced Photo-Fenton Degradation of Tetracycline Using TiO<sub>2</sub>-Coated  $\alpha$ -Fe<sub>2</sub>O<sub>3</sub> Core-Shell Heterojunction. *J. Ind. Eng. Chem.* 68, 14–23. doi:10.1016/j.jiec.2018.07.024
- Zhu, X.-D., Wang, Y.-J., Sun, R.-J., and Zhou, D.-M. (2013). Photocatalytic Degradation of Tetracycline in Aqueous Solution by Nanosized TiO<sub>2</sub>. *Chemosphere* 92 (8), 925–932. doi:10.1016/j.chemosphere.2013.02.066

Zyoud, A., Jondi, W., AlDaqqah, N., Asaad, S., Qamhieh, N., Hajamohideen, A., et al. (2017). Self-sensitization of Tetracycline Degradation with Simulated Solar Light Catalyzed by ZnO@montmorillonite. *Solid State. Sci.* 74, 131–143. doi:10.1016/j.solidstatesciences.2017.09.009

**Conflict of Interest:** The authors declare that the research was conducted in the absence of any commercial or financial relationships that could be construed as a potential conflict of interest.

**Publisher's Note:** All claims expressed in this article are solely those of the authors and do not necessarily represent those of their affiliated organizations, or those of

the publisher, the editors and the reviewers. Any product that may be evaluated in this article, or claim that may be made by its manufacturer, is not guaranteed or endorsed by the publisher.

*Copyright © 2021 Jalloul, Keniar, Tehrani and Boyadjian. This is an open-access article distributed under the terms of the Creative Commons Attribution License (CC BY). The use, distribution or reproduction in other forums is permitted, provided the original author(s) and the copyright owner(s) are credited and that the original publication in this journal is cited, in accordance with accepted academic practice. No use, distribution or reproduction is permitted which does not comply with these terms.*